
PROFESSOR BO YANG (Orcid ID : 0000-0002-0421-3754)

DR JIAN-XIANG LIU (Orcid ID : 0000-0003-0791-1301)

DR MICHAEL K. DEYHOLOS (Orcid ID : 0000-0003-4205-3891)

PROFESSOR YUAN-QING JIANG (Orcid ID : 0000-0003-1367-922X)

Article type : Original Article

Article type: Original Article

Ectopic overexpression of a membrane-tethered transcription factor gene *NAC60* from oilseed rape positively modulates programmed cell death and age-triggered leaf senescence

Jingli Yan^{1a}, Qinqin Chen¹, Xing Cui¹, Peiyu Zhao¹, Shidong Gao¹, Bo Yang^{1*}, Jian-Xiang Liu², Tiantian Tong¹, Michael K. Deyholos³, Yuan-Qing Jiang^{1*}

1. State Key Laboratory of Crop Stress Biology for Arid Areas and, College of Life Sciences, Northwest A & F University, Yangling, Shaanxi 712100, China

2. State Key Laboratory of Plant Physiology and Biochemistry, College of Life Sciences, Zhejiang University, Hangzhou, Zhejiang 310027, China

3. Department of Biology, University of British Columbia, Okanagan Campus, Kelowna, BC, V1V 1V7, Canada

a. Present address: College of Plant Protection, Henan Agricultural University, Zhengzhou, 450002, Henan, China

* Co-corresponding authors:

E-mails: yangwl@nwfau.edu.cn (ORCID: 0000-0002-0421-3754); jiangyq@nwfau.edu.cn

This article has been accepted for publication and undergone full peer review but has not been through the copyediting, typesetting, pagination and proofreading process, which may lead to differences between this version and the [Version of Record](#). Please cite this article as [doi: 10.1111/TPJ.15057](#)

This article is protected by copyright. All rights reserved

(ORCID: 0000-0003-1367-922X)

Fax: 86-29-87092262

Running title: Oilseed rape NAC60 modulates PCD and leaf senescence

Key words

NAC transcription factor, programmed cell death, leaf senescence, oilseed rape, reactive oxygen species

Summary (249 words)

Senescence is an integrative final stage of plant development that is governed by internal and external cues. The NAC (NAM, ATAF1/2, CUC2) transcription factor (TF) family is specific to plants and membrane-tethered NAC TFs (MTTFs) constitute a unique and sophisticated mechanism in stress responses and development. However, the function of MTTFs in oilseed rape (*Brassica napus* L.) remains unknown. Here, we report that BnaNAC60 is a MTTF associated with endoplasmic reticulum (ER) membrane. Expression of *BnaNAC60* was induced during the progression of leaf senescence. Translocation of BnaNAC60 into nuclei was induced by ER stress and oxidative stress treatments. It binds to the NTLBS motif, rather than the canonical NAC recognition site (NACRS). Overexpression of *BnaNAC60* devoid of transmembrane domain, but not the full-length *BnaNAC60*, induces significant ROS accumulation and hypersensitive response (HR)-like cell death in both tobacco and oilseed rape protoplasts. Moreover, ectopic overexpression *BnaNAC60* devoid of transmembrane domain, but not the full-length *BnaNAC60*

in *Arabidopsis* also induces precocious leaf senescence. Furthermore, screening and expression profiling identified an array of functional genes that are significantly induced by *BnaNAC60* expression. Further it was found that *BnaNAC60* can activate the promoter activities of *BnaNYC1*, *BnaRbohD*, *BnaBFN1*, *BnaZAT12* and multiple *BnaVPEs* in a dual-luciferase reporter assay. Electrophoretic mobility shift assay (EMSA) and chromatin immunoprecipitation coupled to quantitative PCR (ChIP-qPCR) assays revealed that *BnaNAC60* directly binds to the promoter regions of these downstream target genes. To summarize, our data show that *BnaNAC60* is a MTF that modulates cell death, ROS accumulation and leaf senescence.

Introduction

Leaf senescence is the last stage of leaf development characterized by leaf yellowing and massive programmed cell death (PCD) (Thomas, 2013). Leaf senescence plays an important role in crop yield determination as many nutrients are relocated from senescent leaves to young leaves or storage organs (Woo *et al.*, 2013). Leaf senescence is not only influenced by endogenous programs such as age, but also by various environmental stresses (Lim *et al.*, 2007). During senescence, leaf cells carry out orderly changes in cell structure, metabolism and gene expression, including degradation of proteins, membrane lipids and nucleic acid (Lim *et al.*, 2007). The most obvious phenotype in aging plants is yellow leaves caused by the degradation of chlorophyll (Hortensteiner, 2006). Some chlorophyll catabolic genes (CCGs) have been identified in the last decade or so, such as *NYC1* (*Non-Yellow Coloring 1*, encodes a Chl b reductase) and *SGR1* (*Stay Green 1*, also known as *NYE1*, *Non-Yellowing 1*), which are critical regulators of chlorophyll degradation (Sato *et al.*, 2009). Besides chlorophylls, leaf senescence is also induced by increased expression of different enzymes that hydrolyze many other macromolecules (Lim *et al.*, 2007). Genes encoding these catabolic enzymes, along with many other genes coding for proteins implicated in nutrient recycling are among the hundreds of senescence-associated genes (SAGs) that are induced during senescence (Gan and Amasino, 1997, He and Gan, 2002, Gepstein *et al.*, 2003, Guo *et al.*, 2004). For instance, *AtSAG12* encodes a cysteine protease involved in nitrogen

mobilization during senescence (James *et al.*, 2018). *AtSAG13* encodes a short-chain alcohol dehydrogenase (Weaver *et al.*, 1998). *AtSAG29* codes for a sugar transporter of the SWEET family (Seo *et al.*, 2011), whereas *AtSAG113* encodes a clade A protein phosphatases type 2C (PP2C) (Zhang and Gan, 2012),

A few studies have shown that developmental senescence is also associated with increased ROS (reactive oxygen species) levels, which not only assist in degradation of cellular components for recycling but also play signaling roles in initiating the senescence process (Guo and Gan, 2012, Rogers and Munne-Bosch, 2016, Yang *et al.*, 2018). Hydrogen peroxide (H₂O₂) is a major form of ROS involved in senescence, with ROS being the main by-products of photosynthesis and respiration or other metabolic processes (Mittler, 2017). Respiratory burst oxidase homologue (RBOH) proteins are the major enzymes responsible for ROS production in the apoplast (Suzuki *et al.*, 2011). ROS is tightly linked with both leaf senescence and PCD and positively influence these two processes (Mhamdi and Van Breusegem, 2018). In plants, there are two types of PCD, with one being developmental PCD (dPCD) occurring in the vegetative and reproductive developmental processes and the other environmental stress-induced PCD (ePCD) (Daneva *et al.*, 2016). Although sometimes used interchangeably, leaf senescence shows difference from PCD (Buono *et al.*, 2019). Whereas nutrient remobilization is an active cellular program depending on viability of nuclei and mitochondria, PCD marks the endpoint of the senescence process (Thomas, 2013). At the final stage of leaf senescence, PCD is a typical symptom resulting from the disintegration of plasma and vacuolar membranes (Daneva *et al.*, 2016). Upon the rupture of tonoplast, hydrolytic enzymes including vacuolar processing enzymes (VPEs) are released into the cytoplasm. VPEs are evolutionarily related to and share structural homology to animal caspases and play an important role in PCD (Hatsugai *et al.*, 2004). Both PCD and leaf senescence need to be tightly coordinated and controlled to optimize recuperation of nutrients. However, the transcriptional control of key genes involved in these two processes remains unknown for oilseed rape (*Brassica napus* L.).

Previous studies have demonstrated that many genes are induced during the progress of leaf senescence in *Arabidopsis* (*Arabidopsis thaliana*) (Gepstein *et al.*, 2003, Guo *et al.*, 2004, Woo *et*

al., 2016), which include those encoding transcription factors (TFs) of WRKY and NAC families (Balazadeh *et al.*, 2008, Kim *et al.*, 2016). The NAC (No Apical Meristem, NAM; Arabidopsis Transcription Activation Factor, ATAF; Cup-shaped Cotyledon, CUC) proteins constitute a large family of plant-specific TFs (Olsen *et al.*, 2005). A total of 113 and 140 NAC genes have been identified from Arabidopsis and rice, respectively, which code for proteins which share a conserved DNA-binding NAC domain at the N-terminus, whereas the C-terminal sequences are relative divergent and contain a potential transcriptional regulatory domain (Puranik *et al.*, 2012). A few NAC TFs are found to play important roles in regulating leaf senescence and under some circumstances two or three NACs work together to modulate the same senescence process (Balazadeh *et al.*, 2008, Kim *et al.*, 2016). For instance, ANAC092 (also referred to as ORE1, ORESARA1), AtNAP (ANAC029), ANAC059 (also referred to as ORS1, ORE1 Sister 1) and ANAC016 are positive regulators of leaf senescence (Guo and Gan, 2006, Balazadeh *et al.*, 2010, Balazadeh *et al.*, 2011, Kim *et al.*, 2013, Sakuraba *et al.*, 2015, Sakuraba *et al.*, 2016). ORE1 could directly activate the *CCG* expression and repress the expression of *GLK2* (*Golden2-Like 2*) to accelerate the leaf senescence process (Rauf *et al.*, 2013, Qiu *et al.*, 2015). Moreover, ORE1 interacts with and activates the promoter of *BFN1* (*Bifunctional Nuclease 1*), whose encoded protein modulates nucleic acid breakdown during senescence and PCD (Perez-Amador *et al.*, 2000). JUB1 (JUNGBRUNNEN1, also referred to as ANAC042) and VNI2 (VND-Interacting 2, also referred to as ANAC083) are two negative regulators in leaf senescence, and *JUB1* can be induced by H₂O₂ (Yang *et al.*, 2011, Wu *et al.*, 2012). What's more, it has been reported that NAC TFs also modulate the senescence process in crops such as rice (Liang *et al.*, 2014, Mao *et al.*, 2017), tomato (Ma *et al.*, 2018), soybean (Pimenta *et al.*, 2016) and wheat (Uauy *et al.*, 2006), which ultimately influence the yield. In addition, soybean NAC30 and NAC81 modulate endoplasmic reticulum (ER) and osmotic stress, and induce cell death through a group of VPEs (Mendes *et al.*, 2013). *VPEs* encode cysteine proteinases and have caspase-1-like activities in plants (Hatsugai *et al.*, 2015). However, no such a TF has been identified from oilseed rape.

Among the NAC TFs in higher plants, a few members possess transmembrane domains (TDs) at their C termini, which are called NTM1 (NAC with transmembrane motif 1) or NTLs

(NTM1-like) (Kim *et al.*, 2006, Kim *et al.*, 2007). AtNLTs may be associated with the ER or nuclear membrane (Liang *et al.*, 2015). NLTs are proposed to possess an intriguing activation strategy to ensure rapid transcriptional responses to various stimuli through proteolytic cleavage of TDs (Chen *et al.*, 2008). There are approximately eighteen NLTs in Arabidopsis and five NLTs in rice (Kim *et al.*, 2007, Kim *et al.*, 2010b). NLTs have also been identified in other crop plants including oilseed rape (Le *et al.*, 2011, Wang *et al.*, 2015). It is found that most of the AtNLT genes are induced by abiotic stress, which may also mediate their proteolytic cleavage and nuclear translocation (Kim *et al.*, 2006, Kim *et al.*, 2007, Park *et al.*, 2011, Kim *et al.*, 2012). Recently, several NLTs have been reported to be involved in either mitochondrial retrograde signaling (De Clercq *et al.*, 2013, Ng *et al.*, 2013, Van Aken and Pogson, 2017), unfolded protein response (UPR) (Yang *et al.*, 2014a) or ER-stress-induced PCD (Yang *et al.*, 2014b). However, the function of NLTs in oilseed rape remains unknown.

We previously identified and cloned as many NAC genes as possible from oilseed rape, among which a few encode NLTs (Wang *et al.*, 2015). Here, we report the functional characterization of BnaNAC60, a membrane-tethered NAC TF that positively modulated cell death, ROS accumulation and leaf senescence, likely through regulating the transcription of downstream target genes directly implicated in these processes.

Results

***BnaNAC60* encodes a membrane-tethered transcription factor and its expression is induced in senescing leaves**

Previously, more than 10 NLT genes were cloned from oilseed rape through RT-PCR. *BnaNAC60* was named as it shows the highest similarity to *ANAC060* (At3g44290) among all *ANACs* in Arabidopsis. Further, *BnaNAC60* was mapped onto C subgenome with the locus number being BnaC01g23890D in *B.napus* genome. *BnaNAC60* is predicted to encode a protein of 340 amino acid residues, which contains a conserved NAC domain divided into five subdomains (A-E) and a putative transmembrane domain at its C terminal (Figures 1a, S1). However, *BnaNAC60* is also different from *ANAC060* from Col-0 in that *ANAC060* from Col-0 has no predicted

transmembrane domain (Figure S1). This difference is caused by a single-nucleotide polymorphism (SNP) in Col-0 *ANAC060*, which affects its splicing pattern (Li *et al.*, 2014). Therefore, we were very curious to know and explore the function and underlying mechanism of *BnaNAC60*. A phylogenetic analysis of NTLs from representative plant species showed that *BnaNAC60* is very closely related to *ANAC089* (NTL17) and *ANAC040* (NTL8), belonging to the subclade IV (Figure S2). Among the five *OsNTLs*, *BnaNAC60* shows the highest similarity to *OsNTL3* (*ONAC074*, *Os01g15640*), function of which has not been reported. Interestingly, we did not identify any NTL gene in moss (*Physcomitrella patens*, bryophyte), and spike moss (*Selaginella moellendorffii*, lycophyte), two species of special importance for the study of plant evolution. *P. patens* is a nonvascular plant while *S. moellendorffii* is thought to be the earliest evolved extant vascular land plant (Bowman *et al.*, 2007). The absence of *NTLs* in these two moss plants suggests *NTLs* may exist in higher land plants only.

In order to investigate the subcellular localization of *BnaNAC60*, its full-length coding region (1-340 aa) and a truncated fragment devoid of the putative transmembrane domain *BnaNAC60ΔTM* (1-321 aa) were fused downstream of the *GFP* (*Green Fluorescent Protein*), which was expressed under the control of the cauliflower mosaic virus (CaMV) 35S promoter in leaf cells of *N. benthamiana*. The HDEL-mCherry and NLS (nuclear localization sequence)-mCherry cassettes were co-expressed to indicate the ER and nuclei, respectively. The results showed that most of the GFP-*BnaNAC60* signals were observed in ER which overlapped with those of HDEL-mCherry, while the GFP-*BnaNAC60ΔTM* signals were distributed exclusively in nuclei which overlapped completely with those of NLS-mCherry (Figure 1b). These results suggest that the *BnaNAC60* is a membrane-tethered TF and the full-length is an inactive or dormant form while the truncated form devoid of transmembrane functions in the nucleus. In this aspect, *BnaNAC60* is very different from its ortholog in *Arabidopsis* Col-0, which has no transmembrane domain at all and is targeted to nuclei only (Figure S3) (Liang *et al.*, 2015).

It has been reported that *ANAC089* is a MTTF and that its translocation from membrane to nucleus is induced by ER stress (Yang *et al.*, 2014b). *BnaNAC60* is phylogenetically close to *BnaNAC089* and *ANAC089* (Figure S2). We therefore considered whether *BnaNAC60ΔTM*

could form a heterodimer with BnaNAC89 Δ TM *in vivo* and the results showed that BnaNAC60 Δ TM interacted with BnaNAC89 Δ TM in nuclei (Figure S4).

Translocation of BnaNAC60 was induced by ER stress and oxidative stress treatments

To investigate whether the translocation of BnaNAC60 was induced by ER stress or oxidative stress treatment, *GFP-BnaNAC60*, *GFP* and *GFP-ANAC089* were individually transiently expressed in oilseed rape protoplasts. Among these, *GFP* was used as a negative control, while *GFP-ANAC089* was set up as a positive control. Tunicamycin (Tn) and H₂O₂ were used to induce ER stress and oxidative stress, respectively. The results showed that GFP alone did not show any change after Tn treatment and displayed a cytosol-nucleus distribution as expected (Figure S6a-b). In the mock-treated protoplasts, most of the GFP-BnaNAC60 signals overlapped with those of the ER marker (Figure S6c). After treatment with Tn, green fluorescence signals emitted by GFP-BnaNAC60 were largely found in the nuclei (Figure S6d). The positive control GFP-ANAC089 showed a similar change (Figure S4e-f), which is consistent with the previous report (Yang *et al.*, 2014b). What's more, the expression of some known ER stress-related genes including *BiP* (*Binding Protein*), *CNX1* (*Calnexin 1*) and *PDI* (*Protein Disulfide Isomerase*) were significantly induced in protoplasts transfected with *BnaNAC60* compared with the *GFP* upon ER stress treatment (Figure S6). In addition, translocation of BnaNAC60 was also induced by 10 mM H₂O₂ treatment and a longer duration of treatment rendered a complete nuclear localization of BnaNAC60 (Figure S7).

To further explore the function of *BnaNAC60*, we analyzed its transcript level during leaf development as well as upon stress or hormone treatments through qRT-PCR. The results showed that *BnaNAC60* was significantly induced in early senescent leaves and even higher in late senescent leaves compared with young and mature leaves (Figure 1c). The expression profiling analysis under various treatments showed that *BnaNAC60* was significantly induced by ABA (abscisic acid), PEG8000 (polyethylene glycol 8000), salt, MV (methyl viologen) and cold (4°C) treatments at the 6 and/or 24 h time points; no significant difference was detected upon the other treatments (Figure 1d).

BnaNAC60 positively modulates PCD in tobacco

To investigate the function of *BnaNAC60*, we performed transient overexpression of it in *N. benthamiana* leaves with β -glucuronidase (*GUS*) as the control. We found that expression of *BnaNAC60 Δ TM* led to hypersensitivity response (HR)-like cell death symptoms as early as 3 dpi (days post-infiltration), and the symptoms were more evident at 5 and 7 dpi (Figure S8a). In contrast, *BnaNAC60* expression showed a mild phenotype only. The hypersensitive response (HR) is a plant defense response triggered by pathogen infection, which results in rapid cell death at the site of pathogen ingress and thus confines the spreading of pathogens to distal parts of plants. HR is also a form of PCD that can activate defense for attenuating subsequent attacks (Heath, 2000). Since HR-like cell death is associated with ROS, we performed DAB (3,3'-diaminobenzidine) staining and quantitative assay of H₂O₂ content. It was found that there was more H₂O₂ accumulation in *BnaNAC60*- and *BnaNAC60 Δ TM*-expressing tissues than that of *GUS*, while *BnaNAC60 Δ TM* expression had a more prominent effect than that of *BnaNAC60* (Figure S8b). Malonaldehyde (MDA) is an important indicator of lipid peroxidation as a result of ROS accumulation. Our data showed that the content of MDA in leaf tissues expressing *BnaNAC60 Δ TM* was higher than that of *GUS* control from 5 dpi, while *BnaNAC60* expression led to significantly more MDA until 7 dpi (Figure S8c). Furthermore, an increased ion leakage in tissues overexpressing *BnaNAC60 Δ TM* was detected, which reflected the extent of cell death (Figure S8d). What's more, loss of chlorophyll and production of anthocyanins were detected since they are central indicators in senescing leaves. The concentration of chlorophyll in leaf tissues expressing *BnaNAC60 Δ TM* decreased significantly after 5 dpi, while the content of anthocyanins significantly increased, whereas the expression of *BnaNAC60* caused a more slow and mild change (Figures S8e,f). To substantiate the hypothesis that the *BnaNAC60*-induced leaf senescence was associated with PCD, we employed a TUNEL (terminal deoxynucleotidyl transferase dUTP nick end labeling) assay. The results showed there were evident green signals emitted from fluorescein isothiocyanate (FITC)-labeled nuclear DNA ends from *BnaNAC60*- and *BnaNAC60 Δ TM*-expressing tissues, with more signals detected in the latter than in the former tissues. In contrast, no signal was detected in *GUS*-expressing tissues (Figure S9).

Interestingly, ectopic overexpression of *ANAC060* from Col-0 in tobacco leaves failed to

induce cell death symptoms and ROS production (Figure S10a), and no significant difference in the chlorophyll content and relative conductivity was observed between tissues overexpressing *ANAC060* and *GFP* control (Figure S10b-c). What's more, ectopic overexpression of full length *ANAC060* or *ANAC060ΔTM* from the C24 ecotype in tobacco leaves failed to induce any obvious symptom (Figure S11). However, we found that ectopic overexpression of *ANAC089ΔTM*, but not full-length *ANAC089*, in tobacco leaves induced hypersensitive response-like cell death symptoms and caused chlorophyll degradation and increased relative conductivity (Figure S12).

BnaNAC60* positively modulates leaf senescence in *Arabidopsis

Next, we expressed *BnaNAC60ΔTM* in *Arabidopsis* plants under the driving of a constitutive CaMV35S promoter. Transgenic plants expressing *GFP* were prepared at the same time and were used as the control. Two independent homozygous transgenic overexpression lines OE-28# and OE-31# were selected from over 30 independent lines for further analyses. qRT-PCR analysis showed that OE-28# and OE-31# lines expressed the *BnaNAC60ΔTM* at approximately 1300- and 500-fold, respectively, compared to that in the *GFP* control line (Figure S13a). Western blot analysis showed that *BnaNAC60ΔTM* protein was successfully expressed in these two overexpression lines (Figure S13b). The OE-28# and OE-31# lines showed accelerated leaf senescence compared with the *GFP* control line under normal growth conditions at 35 and 40 dps (days post-stratification) (Figures S13c, 2a). No significant difference in flowering time was observed on *BnaNAC60ΔTM* –overexpressing plants, though *ANAC089 ΔC*- overexpressing plants show a delayed flowering phenotype (Li *et al.*, 2010). We also examined the level of H₂O₂ by DAB staining and quantitative measurement. Rosette leaves of these two OE lines were more strongly stained than those of the control plant (Figure 2a). A quantitative assay of H₂O₂ contents also supported this (Figure 2b). During the process of leaf senescence, the loss of chlorophyll and an increased ion leakage are two typical physiological features. Rates of chlorophyll loss were faster in OE-28# and OE-31# lines compared with the control (Figure 2c). Moreover, these two OE lines also showed an increased ion leakage at both 35 and 40 dps (Figure 2d).

Moreover, the full-length *BnaNAC60* was constitutively expressed in *Arabidopsis* plants under the driving of CaMV35S promoter as well. Two independent homozygous transgenic

overexpression lines OE-14# and OE-26# were selected for the phenotypic analysis. The successful expression of *BnaNAC60* was confirmed in these two OE lines by qRT-PCR and immunoblotting (Figure S14a-b). A phenotypic assay showed that there was no significant difference between the *GFP* control plant and *BnaNAC60*-overexpression lines at either 35 or 40-d old (Figure S14c). The chlorophyll content and relative conductivity were also similar among these lines (Figure S14d-e).

We also examined the leaf senescence phenotype of these *BnaNAC60*-OE lines in comparison with control, under dark treatment. To do this, age-matched mature rosette leaves were covered with aluminium foil for dark treatment and the plants were kept under normal growth conditions for 2 or 4 d. The results showed that the *BnaNAC60**ATM*-OE lines OE-28# and OE-31# showed earlier senescence than the control plants after dark treatment (Figure S15a, c), whereas the *BnaNAC60*-overexpressing lines OE-14# and OE-26# did not show any significant difference compared with the control plants (Figure S15b, d).

Since the *BnaNAC60**ATM*-OE lines in *Arabidopsis* showed a precocious leaf senescence phenotype and ROS accumulation, we analyzed the expression of an array of marker genes related to chlorophyll degradation, ROS production, cell death and senescence. qRT-PCR was performed with rosette leaves of OE-28# and OE-31# lines as well as the control *GFP* transgenic line at 40 dps. The results showed that *AtSAG12* was highly induced in these two overexpression lines; *AtSAG13* was significantly induced in OE-31#; *AtSAG113* was also significantly induced in the two overexpression lines, whereas *AtSAG29* showed no significant increase in the two OE lines (Figure 2e). *AtNYC1* expression was increased by 2-fold, consistent with the loss of chlorophyll in these two OE lines. What's more, *AtRbohD* and *AtRbohF* which are responsible for apoplastic ROS production (Marino *et al.*, 2012), were also induced, though the magnitude was not large. *AtZAT12*, encoding a zinc-finger transcription factor involved in ROS metabolism (Davletova *et al.*, 2005), was significantly induced in OE-31#. *AtBFN1*, encoding a bifunctional nuclease involved in nucleic acid degradation and leaf senescence (Perez-Amador *et al.*, 2000), was significantly induced (Figure 2e). In contrast, *AtGLK2* (*Golden2-Like 2*), encoding a TF positively regulating chloroplast development (Waters *et al.*, 2008), was significantly repressed in these two

OE lines (Figure 2e). The transcript abundance of these marker genes in *BnaNAC60*-overexpression lines OE-14# and OE-26# was analyzed as well. It can be seen that most of these marker genes showed no significant change, though *AtSAG12*, *AtSAG13*, *AtZAT12* and *AtBFN1* were slightly induced (Figure S14f).

***BnaNAC60* modulates cell death and ROS accumulation in oilseed rape**

To explore the function of *BnaNAC60* in oilseed rape, the full-length *BnaNAC60* as well as *BnaNAC60ΔTM* were transiently expressed in protoplasts of oilseed rape, which is a rapid and efficient system to study the function of a gene (Kaneda *et al.*, 2009). Plasmids expressing *GFP* or *GUS* gene were used as control. To confirm these genes were successfully expressed in protoplasts, we observed the GFP fluorescence and detected their abundance by immunoblotting assay and, the results were all expected (Figure S16a,b). We subjected the transfected protoplasts to various stainings. Initially, live cells cannot be stained by Evans blue, and only dead cells can be stained with dark-blue color. It can be seen that more protoplasts transfected with *BnaNAC60* or *BnaNAC60ΔTM* plasmids were stained with Evans blue dye than in the *GFP* control (Figure 3a). A quantitative comparison showed that death rates of protoplasts transfected with *BnaNAC60ΔTM* and *BnaNAC60* were over 4-fold and 3-fold higher than that of the control, respectively (Figure 3c). Secondly, fluorescein diacetate (FDA) is a fluorescent dye for detecting living cells, only live cells stained with FDA can emit fluorescence. The FDA staining verified that 30.5% and 13.9% of protoplasts transfected with *BnaNAC60ΔTM* and *BnaNAC60* plasmids were dead respectively, which were significantly higher than that of control (Figure 3b, d). In addition, a ROS-specific fluorescence dye, H₂DCFDA(2',7'-dichlorodihydrofluorescein diacetate), was used to detect the accumulation of ROS. We found that protoplasts transfected with *BnaNAC60ΔTM* and *BnaNAC60* plasmids showed stronger fluorescence than that of control (Figure 3e). These results collectively demonstrated that *BnaNAC60* positively modulates cell death and ROS accumulation in oilseed rape too.

***BnaNAC60* binds to a *cis*-element sequence other than NACRS**

Next, we were curious to identify the direct target genes of *BnaNAC60* to better understand its function. One prerequisite is to identify the *cis*-element bound by *BnaNAC60*. Previous work on

the recognition sites of representative ANAC TFs has identified a couple of sites for several NACs (Lindemose *et al.*, 2014). Specifically, members of the stress-responsive NAC (SNAC) subfamily were previously shown to bind to consensus TTNCGT(G/A) (NAC recognition sequence, NACRS) motif in the promoters of target genes (Puranik *et al.*, 2012). It has also been reported that the putative binding element for NTL8/ANAC040 is TTNCTT (Lindemose *et al.*, 2014), which was named NTLBS in this study. A phylogenetic analysis of BnaNAC60 indicated it was clustered together with NTL8 (Figure S2). We therefore hypothesized that BnaNAC60 may be able to recognize and bind to this element too. To test this, we conducted a dual luciferase (LUC) reporter assay. Five tandem repeats of TTNCTT sequences named 5xNTLBS were synthesized and inserted, together with the CaMV35S minimal promoter upstream of the firefly *LUC* gene (Figure 4a). The *Renilla Luciferase (REN)* gene driven by the CaMV35S promoter was co-expressed as an internal control. The full-length *BnaNAC60* and active *BnaNAC60ΔTM* were driven by CaMV35S promoter and used as the effectors with *GUS* used as the control. The results showed that *BnaNAC60ΔTM*, but not *BnaNAC60*, strongly activated the 5xNTLBS-35Smin controlled *LUC* expression with LUC/REN ratios significantly increased compared with the *GUS* control at two time points (Figure 4b). In contrast, neither *BnaNAC60* nor *BnaNAC60ΔTM* significantly activated the expression of *LUC* under the driving of NACRS-35Smin promoter (Figure S17), suggesting that NACRS is not a *cis*-element recognized by *BnaNAC60*.

To confirm the binding of *BnaNAC60* to NTLBS, an electrophoretic mobility shift assay (EMSA) was performed. For this purpose, glutathione S-transferase (GST)-*BnaNAC60ΔTM* fusion protein was purified from *E. coli*. An examination of the purity indicated it was sufficient, with predicted molecular weight (Figure S18). 5xNTLBS probes were labeled with biotin. GST alone was also expressed and purified independently to be used as a control. As shown in Figure 4c, GST-*BnaNAC60ΔTM* bound to 5xNTLBS forming a DNA-protein complex, which migrated more slowly than free probes. When unlabeled DNA fragments were added in excess, the signal intensity of shifted band was strongly reduced. Collectively, these data indicate that *BnaNAC60ΔTM* binds NTLBS directly and specifically.

BnaNAC60 modulates the expression of genes related to cell death, ROS, senescence and

defense

In order to explore the molecular mechanism underlying the function of *BnaNAC60*, we performed qRT-PCR to examine the expression of an array of marker genes involved in PCD, ROS accumulation, defense and leaf senescence. To this end, *BnaNAC60* and *BnaNAC60ΔTM* were individually transiently expressed in 10-day-old oilseed rape seedlings, and *GFP* gene was expressed as the control. The results showed that *BnaNAC60* was significantly induced at 1 dpi and 2 dpi in seedlings overexpressing full-length *BnaNAC60*, while it was significantly induced only at 1 dpi in seedlings overexpressing *BnaNAC60ΔTM*. *BnaBFN1* was slightly induced at 1 dpi, but was significantly induced at 2 dpi (Figure 4d). *BnaZAT12* was significantly induced at 1 dpi and was mildly induced at 2 dpi in *BnaNAC60ΔTM*-overexpressing seedlings. Expression of *BnaβVPE* was significantly induced at 1 dpi while *BnaαVPE* and *BnaγVPE* were induced at 1 dpi as well (Figure 4d). Besides, the expression levels of *BnaRbohD* and *BnaRbohF* were examined and both were induced at 1 dpi, with *BnaRbohD* change being significant in *BnaNAC60ΔTM*-overexpressing seedlings (Figure 4d). SAG and PR (Pathogenesis-Related) genes are prominently induced during leaf senescence and hypersensitive response, so the expression of these marker genes was also examined. The results showed *BnaSAG13* and *BnaSAG15* were significantly induced at one or two time points, and *BnaSAG12* was also induced at 2 dpi in *BnaNAC60ΔTM*-overexpressing seedlings; however, *BnaSAG29* was induced only at 1 dpi in *BnaNAC60*-overexpressing seedlings (Figure 4d). *BnaPR1* was significantly induced at 2 dpi, while *BnaPR2* was significantly induced at both time points in *BnaNAC60ΔTM*-overexpressing seedlings only. *BnaCEP1*, similar to *BnaSAG12*, encoding a papain-like cysteine protease involved in tapetal programmed cell death and pollen development (Zhang *et al.*, 2014), was also detected but showed no significant change (Figure 4d). *HIN1* (*Harpin Inducing 1*) or its Arabidopsis ortholog *YLS9* (*Yellow Leaf-Specific 9*), which is highly induced during HR-like cell death and leaf senescence (Zheng *et al.*, 2004) was also analyzed. The result showed that *BnaHIN1* was induced at 1 dpi only (Figure 4d). In addition, we examined two chlorophyll degradation genes *NYC1* and *NYE1* and, the data showed that both *BnaNYC1* and *BnaNYE1* were significantly induced at 1 dpi only (Figure 4d). Overall, the magnitude of increase in transcript

levels in *BnaNAC60*-overexpressing seedlings was much lower than that in *BnaNAC60ΔTM*-overexpressing seedlings.

To further examine the expression changes of these genes, we performed a similar assay using oilseed rape protoplasts. A Western blot assay confirmed the expression of *BnaNAC60ΔTM*, *BnaNAC60* and the *GFP* (control) in protoplasts (Figure S19a). The results showed that the expression of *BnaBFN1*, *BnaαVPE*, *BnaβVPE*, *BnaγVPE*, *BnaRbohD*, *BnaSAG13*, *BnaSAG15* and *BnaNYC1* were significantly induced in the *BnaNAC60ΔTM*-overexpressing protoplasts, while transcripts of these genes did not show any significant change in *BnaNAC60*-overexpressing protoplasts (Figure S19b). These results suggested that *BnaNAC60* mediated ROS accumulation and cell death likely through inducing the expression of some of these key genes.

Given that transient expression of *BnaNAC60* in *N. benthamiana* leaves also caused severe cell death and ROS accumulation (Figure S8), we also examined the changes in transcript abundance of representative marker genes in tobacco to confirm the similarity of *BnaNAC60* function in different expression systems. Most of these marker genes showed significant changes in the *BnaNAC60ΔTM*-overexpressing tissues; however no significant change or much smaller changes were observed in *BnaNAC60*-overexpressing tissues. The *NbRbohB* (ortholog of *RbohD* in Arabidopsis and oilseed rape) was slightly induced at 3 dpi (Figure S20a) and expression of *NbRbohA* (ortholog of *RbohF*) did not show significant change as a result of *BnaNAC60ΔTM* expression. *NbVPE3* was significantly induced at 3 dpi among the four VPE genes examined here. Similarly, none of the three metacaspase (MC) genes showed any difference. *ZEN1* (*Zinnia Endonuclease 1*), which is the homolog of *BFN1* in Arabidopsis involved in PCD of apical bud meristem (Aoyagi *et al.*, 1998), was highly induced in *BnaNAC60ΔTM*-overexpressing tissues, with a fold change of 38 and 42 at 2 and 3 dpi, respectively (Figure S20a). Moreover, *NbSAG12* and *NbSAG101* were also identified to be significantly induced at 2 dpi, and the later encodes an acyl hydrolase involved in senescence (He and Gan, 2002). *NbZAT12* was highly induced at 3 dpi as well (Figure S20b). *NbLDS1* and *NbLOLI*, encoding two antagonistic regulators of cell death and defense (Epple *et al.*, 2003), were induced and repressed, respectively. Lastly, the defense response marker genes *NbPR2*, *NbPR5*, *NbHIN1*, *NbACRE31* and *NbCYP71D20*, which are

induced in HR-like cell death or by pathogen attack (Pontier *et al.*, 1999), were mostly induced by BnaNAC60 Δ TM as well (Figure S20b).

BnaNAC60 positively modulates the promoter activities of genes involved in ROS production, PCD and leaf senescence

The above investigations indicated that some of these induced genes may constitute the regulon of BnaNAC60 and part of them may be direct targets. We therefore performed a dual-luciferase reporter assay to examine the ability of BnaNAC60 and its activation form of BnaNAC60 Δ TM to activate the transcription of these genes. Promoter regions (including 5'UTR) of these marker genes were fused upstream of *LUC* gene, which were used as reporters. The *REN* gene driven by CaMV35S promoter was used as the internal control (Figure 5a). The plasmids expressing BnaNAC60 Δ TM or BnaNAC60 and *GUS* (control) were used as effectors. LUC/REN ratios reflected the ability of BnaNAC60 to transcriptionally activate its putative downstream genes. The results showed that co-expression of BnaNAC60 or BnaNAC60 Δ TM with *ProBnaZAT12:LUC* and *ProBnaBFN1:LUC* significantly increased LUC/REN ratios at 2 and 3 dpi (Figure 5b,h). In addition, LUC/REN ratios of *ProBnaRbohD*, *ProBna γ VPE* and *ProBnaNYE1* reporters increased about two-fold at 3 dpi when BnaNAC60 Δ TM was used as the effector (Figure 5c, f, g). Besides, BnaNAC60 Δ TM significantly induced the expression of *LUC* driven by promoters of *ProBna α VPE*, *ProBna β VPE* and *ProBnaNYC1* compared with the *GUS* control at the two time points (Figure 5d, e, i). In contrast, neither BnaNAC60 nor BnaNAC60 Δ TM increased the activities of *ProBna δ VPE* and *ProBnaRbohF* (Figure S21), suggesting these two genes are not regulated directly by BnaNAC60.

BnaNAC60 binds to promoters of target genes both *in vitro* and *in vivo* through the NTLBS cis-element

To explore whether there was a direct regulatory relationship between BnaNAC60 and the aforementioned putative target genes, we analyzed the promoter regions of *BnaRbohD*, *Bna α VPE*, *Bna β VPE*, *Bna γ VPE*, *BnaNYC1*, *BnaZAT12* and *BnaBFN1*. It was revealed that multiple NTLBS elements [5'TT(N)CTT3' or 5'AAG(N)AA3'] were present in the promoters of these genes (Figure 6a). Next, EMSA was performed to determine the bindings *in vitro*. The results showed

that BnaNAC60 Δ TM bound to F2, F3 and F4 segments of *BnaRbohD* promoter, but not to F1. As for the three *VPE* promoters, BnaNAC60 Δ TM bound to F1, F2 and F4 segments of *ProBna α VPE*, F2 and F3 segments of *ProBna β VPE*, F1 and F2 segments of *ProBna γ VPE*, and no binding was detected with the other labeled probes (Figure 6b). Besides, BnaNAC60 Δ TM bound to four probes of *ProBnaNYC1* except its F5. Moreover, BnaNAC60 Δ TM bound to F1 and F2 segments of *BnaBFN1* promoter, but not to the F3 segment (Figure 6b). Lastly, only F3 segment of *ProBnaZAT12* was bound by BnaNAC60 Δ TM (Figure 6b). As a control, purified GST protein alone did not bind to any of these labeled segments. To further confirm the binding specificity, a competition assay was performed. The results showed when the unlabeled probes were added in excess, the binding shifts became weaker or even disappeared (Figure S22), supporting the conclusion that BnaNAC60 Δ TM binds specifically to the respective fragments of putative target genes *in vitro*.

To further examine whether these genes are direct targets of BnaNAC60 *in vivo*, chromatin immunoprecipitation (ChIP)-qPCR was performed. An antibody specific to the HA epitope tag was used to collect chromatin DNA bound by BnaNAC60 Δ TM. The utility and specificity of anti-HA antibody was examined and it showed a good result (Figure S23a). Agarose gel electrophoresis was also run to assure the quality of chromatin DNA fragments after sonication. As shown in Figure S23b, the size of DNA smear was mostly located between 200 bp and 1 kb, indicating a good quality. Immunoprecipitated chromatin DNA was thus subjected to qPCR analysis. Primers were designed according to the previous EMSA results, and were subjected to PCR amplification and agarose gel electrophoresis examination before used. Primers that did not show good specificity were discarded and designed again before tested further. As a negative control, primers targeting to a region located at least 1 kb far from the binding site were designed, tested and used in parallel (Figure 7a). Our results showed that BnaNAC60 Δ TM significantly enriched P1 through P3 fragments of *BnaRbohD* and *Bna α VPE* promoters, P1 and P2 fragments of *Bna β VPE*, *Bna γ VPE* and *BnaBFN1* promoters, P1 fragment of *BnaZAT12* promoter, as well as P1 through P5 fragments of *BnaNYC1* promoter (Figure 7b). In contrast, no significant enrichment of control fragments (CK) was detected for any of these seven genes. Collectively, these results

indicate that the active form of BnaNAC60 binds to the promoter of ROS production, PCD and leaf senescence-related genes via the consensus NTLBS sequence.

Discussion

Leaf senescence is a highly coordinated process influenced by the massive reprogramming of gene expression through the action of transcription factors (Kim *et al.*, 2016). Investigation and illumination of the mechanisms modulating plant senescence have great potential for improving crop yield, stress tolerance and nutritional quality (Uauy *et al.*, 2006, Rivero *et al.*, 2007). NAC TFs are plant specific and play diverse roles in plant development, abiotic and biotic stress responses as well as leaf senescence (Olsen *et al.*, 2005, Puranik *et al.*, 2012). A few members of NAC family have been reported to positively or negatively modulate leaf senescence in Arabidopsis, rice, tomato, wheat and cabbage (Guo and Gan, 2006, Balazadeh *et al.*, 2010, Balazadeh *et al.*, 2011, Wu *et al.*, 2012, Kim *et al.*, 2013, Liang *et al.*, 2014, Mahmood *et al.*, 2016, Oda-Yamamizo *et al.*, 2016, Pimenta *et al.*, 2016, Mao *et al.*, 2017, Fan *et al.*, 2018, Ma *et al.*, 2018). Despite the importance in understanding how developmental and environmental signals are integrated to modulate leaf senescence in oilseed rape, the transcriptional control of leaf senescence in this important crop plant remains poorly understood.

In this study, we demonstrated that a membrane-tethered NAC60 in oilseed rape is involved in age-dependent leaf senescence and may integrate the stress signals, ROS signaling and PCD with an inner natural leaf senescence program through activating different but related target genes. BnaNAC60 is associated ER and can be induced by ER and oxidative stresses to translocate to nuclei (Figures 1b, S5, S7). In this aspect, BnaNAC60 is very different from its ortholog in Arabidopsis Col-0, which has no transmembrane domain at all and is targeted to nuclei only (Figure S3) (Liang *et al.*, 2015). BnaNAC60 is phylogenetically close to ANAC089 (Figure S2), an NTL previously reported to modulate ER-stress-induced PCD in Arabidopsis (Yang *et al.*, 2014b). Consistently, BnaNAC60 showed an ability to activate the expression of several unfolded protein response marker genes under ER stress condition (Figure S6), which is, to some degree, different from ANAC089 (Yang *et al.*, 2014b).

What's more, a transient heterologous expression of *ANAC060* from Col-0 in tobacco leaves

indicated that ANAC060, unlike BnaNAC60, failed to induce ROS accumulation or HR-like cell death (Figure S10). A previous report indicates ANAC060 from C24 ecotype is different from that in Col-0 ecotype in that ANAC060 from C24 is an NTL and, this shorter version of the ANAC060 protein is found in ca. 12% of natural Arabidopsis accessions (Li *et al.*, 2014). A quantitative comparison of identifies indicates that BnaNAC60 is more similar to ANAC060 (C24, with an identity of 87.5%) than to ANAC060 (Col-0, 84.2% identity). However, different from BnaNAC60, ectopic overexpression of neither *ANAC060* nor *ANAC060ΔTM* from C24 induced any significant cell death or ROS accumulation (Figure S11). These results suggest that function of ANAC060 is different from that of BnaNAC60, at least in terms of ROS, PCD and leaf senescence, though ANAC060 from C24 is more similar to BnaNAC60, at least in amino acid sequence. An examination of the domain of ANAC060 from Col-0 suggests that it is likely still functional as it contains the typical domains of a regular NAC TF, including a N-terminal NAC domain harboring five subdomains (A, B, C, D, E) and C-terminal transcriptional regulatory domain (Fig S1).

NTLs are usually inactive or in a dormant state through association with cellular membrane system via their transmembrane domains (Kim *et al.*, 2010a). Upon internal and environmental stimuli, NTLs could be activated through proteolytic cleavage either by membrane-associated proteases or by ubiquitination-dependent proteasome activities (Kim *et al.*, 2010a). This constitutes an intriguing mechanism of ensuring rapid transcriptional responses to internal and environmental changes as transcriptional and translational regulations are skipped (Chen *et al.*, 2008, Seo *et al.*, 2008). Although the mechanisms of a few NTLs in Arabidopsis entering nuclei have been explored (Seo *et al.*, 2010, Kim *et al.*, 2010a), for instance, ANAC017 may be cleaved by a rhomboid protease (Ng *et al.*, 2013), there is no uniform pathway for all NTLs. Previous studies have shown that a rising level of endogenous ROS induced by various environmental stresses such as drought, salt and extreme temperatures as well as some developmental changes, can induce leaf senescence and cell death (Khanna-Chopra, 2012, Lee *et al.*, 2012, Woo *et al.*, 2013). Accumulation of ROS can cause protein and lipid dysfunction as well as chlorophyll degradation, which are typical syndromes accompanied with leaf senescence (Lim *et al.*, 2007).

We found that tunicamycin and H₂O₂ treatments triggered membrane release of BnaNAC60 (Figures S5, S7), indicating that the activity of BnaNAC60 is mediated by controllable membrane release and follow-up nuclear localization, which ensures rapid adaptation responses to environmental changes and the progression of leaf senescence. Stress-induced activation of membrane-tethered NAC proteins have been reported with NTL4 (ANAC053), NTL6 (ANAC062) and NTL17 (ANAC089) in *Arabidopsis* (Seo *et al.*, 2010, Lee *et al.*, 2012, Yang *et al.*, 2014a, Yang *et al.*, 2014b).

The expression of *BnaNAC60* was induced during leaf senescence (Figure 1c), suggesting that the function of it may be linked to the age-dependent leaf senescence program. *BnaNAC60* was also induced by a set of environmental stresses and phytohormones, including drought, salt, ABA, and MV (Figure 1d), which are generally positively involved in leaf senescence. To substantiate the role of BnaNAC60, we provided several lines of evidences to support that it plays a positive role in natural leaf senescence. Initially, we demonstrated that constitutive overexpression of the activated form of *BnaNAC60* (i.e. *BnaNAC60ΔTM*), accelerates leaf senescence, which was reflected in quite a few hallmarks such as leaf yellowing, H₂O₂ accumulation, chlorophyll degradation, ion leakage, and increased expression of senescence- and PCD-associated marker genes (Figures 2, S13). We further showed that transient expression of *BnaNAC60* in leaves of tobacco also led to a similar phenotype with phenotype of *BnaNAC60* being much weaker than that of *BnaNAC60ΔTM*, as indicated by the measurements of relevant physiological indices (Figure S8). The function of *BnaNAC60* in protoplasts of oilseed rape was also tested and showed expected results (Figure 3), which is highly similar to rice *NAC4* (Kaneda *et al.*, 2009). Different from SNAC-type NAC TFs, BnaNAC60 showed great affinity towards the NTLBS element (Figure 4), but not towards the NACRS element (Figure S17). Furthermore, screenings of a collection of marker genes related to ROS, PCD, defense responses, and leaf senescence via qRT-PCR and dual-LUC reporter techniques revealed that BnaNAC60 may modulate the transcription of multiple genes from this collection (Figures 2e, 4d, 5, S19, S20). We also observed that *ProBnaZAT12:LUC* and *ProBnaBFN1:LUC* were activated by both BnaNAC60 and BnaNAC60ΔTM, which suggests the regulatory effect of BnaNAC60 and BnaNAC60ΔTM on

different promoters is different, as a basal level of proteolytically processed, activated BnaNAC60 proteins is expected to exist in cells. Through *in vitro* EMSA and *in vivo* ChIP-qPCR techniques, we showed that the active form of BnaNAC60 bound directly to the promoter regions of *BnaRbohD*, *BnaaVPE*, *BnaβVPE*, *BnayVPE*, *BnaNYC1*, *BnaBFN1* and *BnaZAT12* (Figures 6, 7, S22). Thus, this study has built a direct link of BnaNAC60 function with genes whose encoded proteins participate in ROS production, PCD and chlorophyll degradation.

Among the target genes, *RbohD* is responsible for ROS production in many processes including pathogen infection (Torres *et al.*, 2002). As ROS level has to be tightly restrained to avoid detrimental consequence on plant cells, *RbohD* is modulated not only by post-translational phosphorylation but also under transcriptional control by TFs (Kadota *et al.*, 2015). Previously, it was reported that *RbohC* and *RbohE* are regulated by transmembrane motif 1-like 4 (NTL4, also referred to as ANAC053) to mediate drought-induced leaf senescence (Lee *et al.*, 2012). This indicates that different NTLs may target different members of *Rboh* gene family. *ZAT12* is a member of the C2H2-type plant-specific zinc finger transcription factor family and its expression is induced by many different types of abiotic stresses including oxidative stress; *ZAT12* is also required for the up-regulation of many ROS signaling genes (Rizhsky *et al.*, 2004, Davletova *et al.*, 2005). Here, we identified *BnaZAT12* as a direct target of BnaNAC60 and expression of *BnaZAT12* is induced by BnaNAC60.

Interestingly, we also found that BnaNAC60 targeted multiple VPE genes, indicative of the execution of a cell death program. VPEs are cysteine proteases exhibiting caspase-like activity (Hara-Nishimura *et al.*, 2005). Originally found to be responsible for the maturation of seed storage proteins and vacuolar proteins, VPEs have also been shown to trigger vacuolar collapse-mediated PCD during defense response and development (Hatsugai *et al.*, 2004). Here, we reported that overexpression of the activated form of *BnaNAC60* led to premature leaf senescence, cell death and up-regulation of *VPEs* (Figures 4, S19), suggesting activation of VPE and developmental PCD play a role in this process. De-greening of leaves as a consequence of chlorophyll degradation, is a characteristic of leaf senescence (Hortensteiner and Krautler, 2011). *NYC1* is a Chl b reductase catalyzing the step one of Chl degradation (Horie *et al.*, 2009).

Overexpression of *BnaNAC60ΔTM* promoted *NYC1* expression and trans-activated its promoter (Figures 2e, 4d, 5h, S19). More recent studies demonstrated that ANAC019/055/072 can directly promote the expression of three *CCGs* (*NYE1*, *NYE2* and *NYC1*) in JA-triggered Chl degradation (Zhu *et al.*, 2015); ORE1 (ANAC092) also activates the expression of *CCGs* in ethylene-triggered Chl degradation (Qiu *et al.*, 2015); ANAC016 can directly induce *NYE1* transcription (Sakuraba *et al.*, 2016), and ANAC046 positively modulates the expression of *CCGs* and leaf senescence (Oda-Yamamizo *et al.*, 2016). These data suggest that distinct NACs could be recruited individually or together to ensure a temporally and spatially coordinated regulation of Chl degradation leading to leaf senescence through different signaling pathways in different scenarios.

BFNI is among the genes that are positively regulated by BnaNAC60 (Figures 2e, 4d, 5i, S19). It encodes a type I nuclease responsible for the degradation of RNA and single-stranded DNA during several growth and developmental processes, sharing high similarity to *ZEN1* that is associated with PCD in *Zinnia elegans* (Ito and Fukuda, 2002). *BFNI* expression was found to be specifically increased during leaf and stem senescence (Perez-Amador *et al.*, 2000). In addition, *BFNI* is also specifically expressed in the leaf and fruit abscission zones, suggesting an involvement in developmental PCD (Farage-Barhom *et al.*, 2008). In plants, age-induced dPCD occurs in all cell types of organs or even whole plants as the end point of plant senescence (Daneva *et al.*, 2016). Previously, ORE1 has been found to target *BFNI* to modulate leaf senescence in Arabidopsis (Matallana-Ramirez *et al.*, 2013). However, the binding site of ORE1 is obviously different from that of BnaNAC60 (Figures 6, 7), suggesting *BFNI* could be regulated by distinct NAC TFs as well.

In conclusion, this study has revealed an ER membrane-tethered NAC transcription factor NAC60 from oilseed rape that acts as an upstream regulator of ROS accumulation, cell death and leaf senescence, likely through activating the expression of ROS-generating *RbohD*, ROS signaling gene *ZAT12*, developmental PCD-associated *VPEs* and *BFNI*, as well as Chl degradation-related *NYC1* genes (Figure S24).

Experimental procedures

Plant materials and growth conditions

Seeds of oilseed rape (*Brassica napus*), tobacco (*Nicotiana benthamiana*) and Arabidopsis (Col-0 and C24) were surface sterilized for 1 min in 70% ethanol and then in 2.6% bleach solution (containing 0.01% Tween-20) for 2-4 min, before washed for 4-5 times in sterile de-ionized water. The seeds were stratified for 2 days at 4 °C and germinated on 1/2 MS (Murashige and Skoog) medium (Caisson labs, USA, <https://www.caissonlabs.com/>) at 22 °C in a greenhouse with 14 h light/10 h dark photoperiod. 7-day-old seedlings were transplanted to soil or used in other experiments.

Stress treatments and quantitative RT-PCR (qRT-PCR)

7-day-old seedlings of oilseed rape were transferred onto 1/2 MS medium supplemented with different hormones or other chemicals with normal 1/2 MS medium used as the control. For the cold and heat treatments, seedling plates were placed in 4 °C fridge and 38 °C chamber, respectively. Leaf tissues at different developmental stages were harvested at specific time points (Yan *et al.*, 2018). The whole process was repeated three times independently to prepare three biological replicates. Total RNA was extracted using a plant RNA kit (Omega Bio-tek, USA, <https://www.omegabiotek.com/>) and was treated with DNaseI (Ambion, USA, <https://www.thermofisher.com/>). cDNA synthesis was performed using 5 µg total RNA and RNaseH- M-MLV (Takara, Japan, <https://www.takarabiomed.com.cn/>). qRT-PCR was performed using SYBR GreenI premix (CWbio, China, <https://www.cwbiotech.com/>) on the CFX96 real-time system (Bio-Rad, USA, <https://www.bio-rad.com/>) with the following program, 10 min at 95 °C, 35 cycles of 95 °C for 15 s and 60 °C for 1 min. Gene-specific primers were designed using PrimerSelect or Primer 3. The specificity and amplification efficiency were examined by BLAST and melting curve analyses. The reference genes used were *BnaUP1* and *BnaUBC9* for oilseed rape (Chen *et al.*, 2010), *AtUBC21* and *AtUBQ10* for Arabidopsis (Czechowski *et al.*, 2005). Relative expression levels (fold changes) were calculated according to a previous formula (Pfaffl, 2001).

Subcellular localization assay

The coding regions (CDS) of *BnaNAC60* (FL, full-length) and *BnaNAC60ΔTM* (deleted

transmembrane domain) were amplified and fused downstream of a green fluorescent protein (GFP) gene in the p35SNGFP binary vector, which was modified from pCsGFPBT (GenBank Acc No DQ370426). *Agrobacterium tumefaciens* GV3101 were transformed with these constructs through a freeze-thaw method. Leaves of 28-day-old *N. benthamiana* were infiltrated and the GFP signals were detected after two days on a confocal microscope (Olympus, Japan, <https://www.olympus-global.com/>). The HDEL-mCherry marker (CD3-959) was described previously (Nelson *et al.*, 2007).

Plant transformation and leaf senescence assay

The CDSs of *BnaNAC60* and *BnaNAC60ΔTM* were subcloned into pHFGFP and pYJGFP binary vectors, respectively, which were modified from pCsGFPBT. Recombinant plasmids were introduced into *A. tumefaciens* GV3101, which was then used to transform WT *A. thaliana* (Col-0) plants via the floral dip method (Clough and Bent, 1998). Putative transformants (T1) were selected by placing seeds on agar-solidified 1/2 MS medium containing 25 mg L⁻¹ hygromycin B (Amresco, USA, <https://www.amresco-inc.com/>). At T3 generation, high expression lines were screened through qRT-PCR. An empty vector pYJGFP carrying *GFP* alone was also transformed into WT *A. thaliana* plants separately. Seeds of homozygous T3 generation and control line grown at the same time under identical standard conditions were used for phenotypic assay (Yang *et al.*, 2018).

Isolation of protoplasts from oilseed rape and transient expression

The expression cassettes (CaMV35S::gene of interest followed with terminator sequence) of individual genes were released from the above recombinant plasmids for overexpression through restriction before ligated into the pUC19 plasmid. Mesophyll cell protoplasts were isolated from the fifth and sixth leaves of 6-week-old oilseed rape plants grown under 14-h light/10-h dark conditions as previously described (Yoo *et al.*, 2007). For 2 × 10⁵ protoplasts, 20 μg of plasmid DNA were transfected into the protoplasts by a PEG4000/CaCl₂-mediated method. Transfected protoplasts were incubated at room temperature in 24-well plates for 14-16 h.

For the membrane-to-nucleus translocation analysis, tunicamycin (Tn, Sigma-Aldrich, USA, <https://www.sigmaaldrich.com/>) was added into transfected protoplasts to a final concentration of

5 $\mu\text{g ml}^{-1}$ and incubated for 6 h. For the H_2O_2 treatment, transfected protoplasts were subjected to 10 mM H_2O_2 (Alfa Aesar, France, <https://www.alfa.com/>) for 15 min and washed once with 1xPBS buffer, before incubated for a further 5 h. Images were taken on a laser confocal microscope (TCS-SP8, Leica, Germany, <https://en.leica-camera.com/>). For the staining, transfected protoplasts were incubated in a 0.05% Evans blue (MP Biomedicals, USA, <https://www.mpbio.com/>) staining buffer for 15 min or in a 0.01% FDA (fluorescein diacetate, MP Biomedicals) staining buffer for 5 min. After washing, images were taken on a fluorescence microscope (DM500B, Leica). Scoring of dead protoplasts was performed by counting 20 individual fields of three replicates. The H_2DCFDA staining were performed as described previously (Yan *et al.*, 2018).

Measurement of hydrogen peroxide (H_2O_2) and DAB staining

About 0.1 g of fresh sample was extracted with 1 ml 5% (w/v) trichloroacetic acid (TCA, Alfa Aesar) buffer. After spinning, the supernatant was neutralized to be pH 7.5 with 1 M NH_4OH (Alfa Aesar). Extract was divided into two aliquots of 100 μl . One aliquot added with catalase (Sigma-Aldrich) was used as the control, and the other aliquot was processed without catalase. Both aliquots were added with 400 μl of 0.1 M Tris-HCl followed with the addition of 500 μl colorimetric reagent. The colorimetric reagent was prepared freshly by mixing 1:1 (v/v) 0.3 mM potassium titanium oxalate (Alfa Aesar) and 0.3 mM resorcinol monosodium salt (Alfa Aesar). Absorbance at 508 nm was measured against a standard curve of H_2O_2 , after incubation at room temperature for 15 min (Patterson *et al.*, 1984). For DAB (MP Biomedicals) staining, the detached leaves were incubated in the DAB staining solution for 4 h at room temperature and decolorized in a destaining solution at 95°C for 15 min (Sun *et al.*, 2014).

Chlorophyll, anthocyanin and malonaldehyde (MDA) content measurements and electrolyte leakage assay

Chlorophyll, anthocyanin and MDA contents were quantified as described previously (Chen *et al.*, 2016). For electrolyte leakage assay, about 0.1 g of leaf tissue was immersed in 5 ml of deionized water. After applying vacuum for 15 min and shaking at 180 rpm for 1 h at 25°C, the electrical conductivity of samples (C1) and deionized water (C0) was determined with an electrical

conductivity meter (Leici, China, <http://www.lei-ci.com/>). Samples were boiled for 15 min and let cool to room temperature, and the electrical conductivity of samples (C2) and deionized water (C0') were determined again. Total relative ion leakage was calculated as per $\%=[(C1-C0)/(C2-C0')]\times 100$.

Dual-luciferase reporter assay

The CDSs of *BnaNAC60* and *BnaNAC60ΔTM* were amplified and inserted into the binary pYJHA vector (modified from pCsGFPBT) and used as effectors. *GUS* cloned into the same empty vector resulting in pYJHA-GUS was used as the control effector. Promoters plus 5'UTR were amplified from genomic DNA using PCR mediated by high-fidelity PrimeSTAR HS DNA polymerase (TaKaRa, Japan). The promoters were inserted into vector pGreenII0800-LUC (Hellens *et al.*, 2005), in which *Renilla luciferase (REN)* under the driving of the 35S promoter was used as the endogenous control. Agrobacterium cultivation and infiltration into leaves of *N. benthamiana* were performed as described previously (Yan *et al.*, 2018). Leaf discs were harvested at 2 and 3 dpi (days post-infiltration). Samples were ground in liquid nitrogen with luciferase activities measured using a Dual-Luciferase Reporter Assay kit (Promega, USA, <https://www.promega.com/>).

Protein purification and electrophoretic mobility shift assay (EMSA)

The CDS of *BnaNAC60ΔTM* was recombined into the pGEX 4T-1 vector, and transformed into *E. coli* strain Rosetta (DE 3) (Novagen, Germany, <http://www.merckmillipore.com>). The fusion protein expression was induced at 25 °C by 0.1 mM IPTG (isopropyl β-D-thiogalactoside, Amresco) for 8 h. Cells were harvested by centrifugation at 12,000 g for 20 min, and lysed by ultrasonication. The supernatant was used for protein purification via GST bind resin (Merck, Germany, <http://www.merckmillipore.com>). Double-stranded probes were either annealed from synthesized single-stranded primers (Sangon, China, <https://www.sangon.com/>) or amplified by the high-fidelity *Pfu* polymerase (Bioer, China, <http://www.bioer.com.cn/>). Primers are listed in Table S1. EMSA was performed using a LightShift chemiluminescent EMSA kit (Thermo Scientific, USA, <https://www.thermofisher.com/>). After binding reactions, samples were loaded into a 5% non-denatured polyacrylamide gel and blotted onto a positively charged nylon

membrane (GE Healthcare, USA, <https://www.gehealthcare.com/>) under UV cross-linking. Signals were detected using the streptavidin-HRP system on a ChemDoc system (Bio-Rad, USA).

Chromatin immunoprecipitation and quantitative PCR (ChIP-qPCR)

The CDS of *BnaNAC60ΔTM* was constructed into an expression vector pUC19-HF in which a CaMV35S promoter was used to drive the expression of *BnaNAC60ΔTM* tagged with sequence coding for 3xHA-3xFLAG tag at its 3' end. ChIP was performed according to (Lee *et al.*, 2017) with minor modifications according to (Saleh *et al.*, 2008). Briefly, 2×10^5 oilseed rape protoplasts were transfected with 20 µg of plasmid DNA and were incubated for 16 h at room temperature before harvested and washed with 1xPBS buffer (pH 7.4) twice. Samples were cross-linked with 1% formaldehyde in 1xPBS for 10 min at room temperature. Afterwards, glycine (MP Biomedicals) was added to a final concentration of 0.1 M to quench the cross-linking reaction. Anti-HA antibody (Sigma-Aldrich) was used for immunopurification of TF-DNA complexes. A sample without HA antibody was used as the control. Isolated chromatin was sheared by sonication to obtain fragment sizes between 200-500 bp. Fragmented genomic DNA was precipitated at the presence of glucogen (Fermentas, USA, <https://www.thermofisher.com/>). qPCR was performed on the immunoprecipitated DNA on the CFX96 thermocycler. Primers were designed by Primer 3 and the control primers were designed so that the amplified regions were located at least 1 kb away from the ATG translation initiation site. Primers are listed in Table S1. The percent of genomic DNA precipitated by HA antibody (ChIP signal) compared with the total input DNA was calculated as follows: $\% \text{ input} = 100 \times 2^{\Delta(Ct(\text{input}) - Ct(\text{sample}))}$ (Kumar and Lucyshyn, 2017).

Statistical analysis

All the data were generated from three to four biological replicates. Statistical analysis was performed by using SPSS (ver 16.0, IBM, USA, <https://www.ibm.com/products/spss-statistics>) software (ANOVA test) and MS Excel 2003 (Student's *t*-test).

Data availability statement

All relevant data can be found within the manuscript and its supporting materials. All the materials

described in the paper will be available on request for any non-profit research.

Acknowledgements

We thank Drs. Jorg Kudla (Universitat Munster, Germany) for providing the BiFC vectors and Zhi-Zhong Gong (China Agricultural University) for providing C24 seeds. We also thank Moyu Dai and Jiangxiao Zhang (NWAUFU) for technical assistance. The work was supported by the National Natural Science Foundation of China [31771699 to Y.Q. J., 31301648 to B.Y.], the Production, Research and Development Program of Yangling [2016CXY-07 to Y.Q.J], the Fundamental Research Funds for the Central Universities [2452017025 to Y.Q.J, 2452019067 to B.Y.] and by the open project of SKLCSBAA (CSBAA2014004 to J.X. L.).

Author contributions

YQJ and BY conceived and supervised the project. YQJ, BY and JY designed the experiments. JY, QC, XC, PZ, SG performed the experiments. TT, PZ and MKD contributed research materials. JY and YQJ analyzed the data. YQJ, JY and BY wrote the manuscript. JXL and MKD helped in analyzing the data and writing the manuscript. YQJ, BY and JXL acquired the funding. All authors read and approved the manuscript.

Conflict of Interest Statement

The authors declare that no competing or conflict of interest exists.

Supporting information

Additional Supporting Information may be found in the online version of this article.

Table S1. Primers used in this study.

Figure S1 Multiple alignment analysis of the BnaNAC60 protein with some typical NAC proteins.

Figure S2 Phylogenetic analysis of BnaNAC60 and NTLs from different species.

Figure S3 Subcellular localization assay of ANAC060 protein in *N.benthamiana*.

Figure S4 Bimolecular fluorescence complementation assay of interaction between

BnaNAC60 Δ TM and BnaNAC89 Δ TM *in vivo*.

Figure S5 Nuclear relocation of GFP-BnaNAC60 in response to ER stress.

Figure S6 Examination of expression of unfolded protein response marker genes upon ER stress treatment.

Figure S7 Nuclear relocation of GFP-BnaNAC60 in response to oxidative stress.

Figure S8 Expression of *BnaNAC60* induced ROS accumulation and cell death in *N.benthamiana* leaves.

Figure S9 Detection of nuclear DNA fragmentation in leaf tissues expressing *BnaNAC60* via TUNEL assay.

Figure S10 Expression of *ANAC60* from Col-0 does not induce cell death and ROS production in *N.benthamiana* leaves.

Figure S11 Expression of *ANAC060* from C24 fails to induce cell death and ROS production in *N.benthamiana* leaves.

Figure S12 Expression of *ANAC089 Δ TM* can induce cell death and ROS production in *N.benthamiana* leaves.

Figure S13 Expression assay of *BnaNAC60 Δ TM* in overexpression lines and phenotypic analysis.

Figure S14 Expression of *BnaNAC60* in overexpression lines and leaf senescence phenotypic analysis.

Figure S15 Phenotypic analysis of *BnaNAC60* transgenic plants in dark-induced leaf senescence.

Figure S16 Subcellular localization and immunoblotting analysis of BnaNAC60 in oilseed rape protoplasts.

Figure S17 A dual luciferase reporter assay of transcriptional control of NACRS elements by BnaNAC60.

Figure S18 Examination of purified GST-BnaNAC60 Δ TM protein via SDS-PAGE.

Figure S19 Expression analysis of cell death-, ROS- and senescence-related marker genes in protoplasts expressing *BnaNAC60* and *BnaNAC60 Δ TM*.

Figure S20 qRT-PCR analysis of the expression of ROS-, cell death- and defense-related marker genes in *N.benthamiana*.

Figure S21 The dual luciferase reporter assay of transactivation of BnaNAC60 towards two oilseed rape genes.

Figure S22 Competitive EMSA assay of binding of BnaNAC60 Δ TM to promoter regions of target genes.

Figure S23 Protein detection and electrophoretic analysis of fragmented chromatin DNA for ChIP-qPCR assay.

Figure S24 A proposed model of BnaNAC60 transcription factor in leaf senescence.

Supporting materials and methods

References

- Aoyagi, S., Sugiyama, M. and Fukuda, H. (1998) BEN1 and ZEN1 cDNAs encoding S1-type DNases that are associated with programmed cell death in plants. *FEBS letters*, **429**, 134-138.
- Balazadeh, S., Kwasniewski, M., Caldana, C., Mehrnia, M., Zanon, M.I., Xue, G.P. and Mueller-Roeber, B. (2011) ORS1, an H₂O₂ - responsive NAC transcription factor, controls senescence in *Arabidopsis thaliana*. *Mol Plant*, **4**, 346-360.
- Balazadeh, S., Riano-Pachon, D.M. and Mueller-Roeber, B. (2008) Transcription factors regulating leaf senescence in *Arabidopsis thaliana*. *Plant Biol (Stuttg)*, **10 Suppl 1**, 63-75.
- Balazadeh, S., Siddiqui, H., Allu, A.D., Matallana-Ramirez, L.P., Caldana, C., Mehrnia, M., Zanon, M.I., Kohler, B. and Mueller-Roeber, B. (2010) A gene regulatory network controlled by the NAC transcription factor ANAC092/AtNAC2/ORE1 during salt-promoted senescence. *Plant J*, **62**, 250-264.
- Bowman, J.L., Floyd, S.K. and Sakakibara, K. (2007) Green genes-comparative genomics of the green branch of life. *Cell*, **129**, 229-234.
- Buono, R.A., Hudecek, R. and Nowack, M.K. (2019) Plant proteases during developmental programmed cell death. *J Exp Bot*, **70**, 2097-2112.
- Chen, B., Niu, F., Liu, W.Z., Yang, B., Zhang, J., Ma, J., Cheng, H., Han, F. and Jiang, Y.Q. (2016) Identification, cloning and characterization of R2R3-MYB gene family in canola (*Brassica napus* L.) identify a novel member modulating ROS accumulation and hypersensitive-like cell death. *DNA Res*, **23**, 101-114.
- Chen, X., Truksa, M., Shah, S. and Weselake, R.J. (2010) A survey of quantitative real-time polymerase chain

reaction internal reference genes for expression studies in *Brassica napus*. *Anal Biochem*, **405**, 138-140.

Chen, Y.N., Slabaugh, E. and Brandizzi, F. (2008) Membrane-tethered transcription factors in *Arabidopsis thaliana*: novel regulators in stress response and development. *Curr Opin Plant Biol*, **11**, 695-701.

Clough, S.J. and Bent, A.F. (1998) Floral dip: a simplified method for *Agrobacterium*-mediated transformation of *Arabidopsis thaliana*. *Plant Journal*, **16**, 735-743.

Czechowski, T., Stitt, M., Altmann, T., Udvardi, M.K. and Scheible, W.R. (2005) Genome-wide identification and testing of superior reference genes for transcript normalization in *Arabidopsis*. *Plant Physiology*, **139**, 5-17.

Daneva, A., Gao, Z., Van Durme, M. and Nowack, M.K. (2016) Functions and regulation of programmed cell death in plant development. *Annu Rev Cell Dev Biol*, **32**, 441-468.

Davletova, S., Schlauch, K., Coutu, J. and Mittler, R. (2005) The zinc-finger protein Zat12 plays a central role in reactive oxygen and abiotic stress signaling in *Arabidopsis*. *Plant Physiol*, **139**, 847-856.

De Clercq, I., Vermeirssen, V., Van Aken, O., Vandepoele, K., Murcha, M.W., Law, S.R., Inze, A., Ng, S., Ivanova, A., Rombaut, D., van de Cotte, B., Jaspers, P., Van de Peer, Y., Kangasjarvi, J., Whelan, J. and Van Breusegem, F. (2013) The membrane-bound NAC transcription factor ANAC013 functions in mitochondrial retrograde regulation of the oxidative stress response in *Arabidopsis*. *Plant Cell*, **25**, 3472-3490.

Epple, P., Mack, A.A., Morris, V.R. and Dangel, J.L. (2003) Antagonistic control of oxidative stress-induced cell death in *Arabidopsis* by two related, plant-specific zinc finger proteins. *Proc Natl Acad Sci U S A*, **100**, 6831-6836.

Fan, Z.Q., Tan, X.L., Chen, J.W., Liu, Z.L., Kuang, J.F., Lu, W.J., Shan, W. and Chen, J.Y. (2018) BrNAC055, a novel transcriptional activator, regulates leaf senescence in Chinese flowering cabbage by modulating reactive oxygen species production and chlorophyll degradation. *J Agric Food Chem*, **66**, 9399-9408.

Farage-Barhom, S., Burd, S., Sonogo, L., Perl-Treves, R. and Lers, A. (2008) Expression analysis of the BFN1 nuclease gene promoter during senescence, abscission, and programmed cell death-related processes. *J Exp Bot*, **59**, 3247-3258.

Gan, S. and Amasino, R.M. (1997) Making Sense of Senescence (Molecular Genetic Regulation and Manipulation of Leaf Senescence). *Plant Physiol.*, **113**, 313-319.

Gepstein, S., Sabehi, G., Carp, M.J., Hajouj, T., Nesher, M.F., Yariv, I., Dor, C. and Bassani, M. (2003)

Large-scale identification of leaf senescence-associated genes. *Plant J.*, **36**, 629-642.

Guo, Y., Cai, Z. and Gan, S. (2004) Transcriptome of Arabidopsis leaf senescence. *Plant, Cell and Environment*, **27**, 521-549.

Guo, Y. and Gan, S. (2006) AtNAP, a NAC family transcription factor, has an important role in leaf senescence. *Plant J.*, **46**, 601-612.

Guo, Y. and Gan, S.S. (2012) Convergence and divergence in gene expression profiles induced by leaf senescence and 27 senescence-promoting hormonal, pathological and environmental stress treatments. *Plant Cell Environ*, **35**, 644-655.

Hara-Nishimura, I., Hatsugai, N., Nakaune, S., Kuroyanagi, M. and Nishimura, M. (2005) Vacuolar processing enzyme: an executor of plant cell death. *Curr Opin Plant Biol*, **8**, 404-408.

Hatsugai, N., Kuroyanagi, M., Yamada, K., Meshi, T., Tsuda, S., Kondo, M., Nishimura, M. and Hara-Nishimura, I. (2004) A plant vacuolar protease, VPE, mediates virus-induced hypersensitive cell death. *Science*, **305**, 855-858.

Hatsugai, N., Yamada, K., Goto-Yamada, S. and Hara-Nishimura, I. (2015) Vacuolar processing enzyme in plant programmed cell death. *Front Plant Sci*, **6**, 234.

He, Y. and Gan, S. (2002) A gene encoding an acyl hydrolase is involved in leaf senescence in Arabidopsis. *Plant Cell*, **14**, 805-815.

Heath, M.C. (2000) Hypersensitive response-related death. *Plant Mol Biol*, **44**, 321-334.

Hellens, R.P., Allan, A.C., Friel, E.N., Bolitho, K., Grafton, K., Templeton, M.D., Karunairetnam, S., Gleave, A.P. and Laing, W.A. (2005) Transient expression vectors for functional genomics, quantification of promoter activity and RNA silencing in plants. *Plant Methods*, **1**, 13.

Horie, Y., Ito, H., Kusaba, M., Tanaka, R. and Tanaka, A. (2009) Participation of chlorophyll b reductase in the initial step of the degradation of light-harvesting chlorophyll a/b-protein complexes in Arabidopsis. *J Biol Chem*, **284**, 17449-17456.

Hortensteiner, S. (2006) Chlorophyll degradation during senescence. *Annu Rev Plant Biol*, **57**, 55-77.

Hortensteiner, S. and Krautler, B. (2011) Chlorophyll breakdown in higher plants. *Biochim Biophys Acta*, **1807**, 977-988.

Ito, J. and Fukuda, H. (2002) ZEN1 is a key enzyme in the degradation of nuclear DNA during programmed cell

death of tracheary elements. *The Plant cell*, **14**, 3201-3211.

James, M., Poret, M., Masclaux-Daubresse, C., Marmagne, A., Coquet, L., Jouenne, T., Chan, P., Trouverie, J. and Etienne, P. (2018) SAG12, a major cysteine protease involved in nitrogen mobilization during senescence for seed production in *Arabidopsis thaliana*. *Plant Cell Physiol.*

Kadota, Y., Shirasu, K. and Zipfel, C. (2015) Regulation of the NADPH Oxidase RBOHD During Plant Immunity. *Plant Cell Physiol*, **56**, 1472-1480.

Kaneda, T., Taga, Y., Takai, R., Iwano, M., Matsui, H., Takayama, S., Isogai, A. and Che, F.S. (2009) The transcription factor OsNAC4 is a key positive regulator of plant hypersensitive cell death. *EMBO J*, **28**, 926-936.

Khanna-Chopra, R. (2012) Leaf senescence and abiotic stresses share reactive oxygen species-mediated chloroplast degradation. *Protoplasma*, **249**, 469-481.

Kim, H.J., Nam, H.G. and Lim, P.O. (2016) Regulatory network of NAC transcription factors in leaf senescence. *Curr Opin Plant Biol*, **33**, 48-56.

Kim, M.J., Park, M.J., Seo, P.J., Song, J.S., Kim, H.J. and Park, C.M. (2012) Controlled nuclear import of the transcription factor NTL6 reveals a cytoplasmic role of SnRK2.8 in the drought-stress response. *Biochem J*, **448**, 353-363.

Kim, S.G., Lee, S., Ryu, J. and Park, C.M. (2010a) Probing protein structural requirements for activation of membrane-bound NAC transcription factors in *Arabidopsis* and rice. *Plant Science*, **178**, 239-244.

Kim, S.G., Lee, S., Seo, P.J., Kim, S.K., Kim, J.K. and Park, C.M. (2010b) Genome-scale screening and molecular characterization of membrane-bound transcription factors in *Arabidopsis* and rice. *Genomics*, **95**, 56-65.

Kim, S.Y., Kim, S.G., Kim, Y.S., Seo, P.J., Bae, M., Yoon, H.K. and Park, C.M. (2007) Exploring membrane-associated NAC transcription factors in *Arabidopsis*: implications for membrane biology in genome regulation. *Nucleic Acids Res*, **35**, 203-213.

Kim, Y.S., Kim, S.G., Park, J.E., Park, H.Y., Lim, M.H., Chua, N.H. and Park, C.M. (2006) A membrane-bound NAC transcription factor regulates cell division in *Arabidopsis*. *Plant Cell*, **18**, 3132-3144.

Kim, Y.S., Sakuraba, Y., Han, S.H., Yoo, S.C. and Paek, N.C. (2013) Mutation of the *Arabidopsis* NAC016 transcription factor delays leaf senescence. *Plant Cell Physiol*, **54**, 1660-1672.

Kumar, S.V. and Lucyshyn, D. (2017) Studying transcription factor binding to specific genomic loci by chromatin

immunoprecipitation (ChIP). *Methods Mol Biol*, **1497**, 193-203.

- Le, D.T., Nishiyama, R., Watanabe, Y., Mochida, K., Yamaguchi-Shinozaki, K., Shinozaki, K. and Tran, L.S.** (2011) Genome-wide survey and expression analysis of the plant-specific NAC transcription factor family in soybean during development and dehydration stress. *DNA Res*, **18**, 263-276.
- Lee, J.H., Jin, S., Kim, S.Y., Kim, W. and Ahn, J.H.** (2017) A fast, efficient chromatin immunoprecipitation method for studying protein-DNA binding in Arabidopsis mesophyll protoplasts. *Plant Methods*, **13**, 42.
- Lee, S., Seo, P.J., Lee, H.J. and Park, C.M.** (2012) A NAC transcription factor NTL4 promotes reactive oxygen species production during drought-induced leaf senescence in Arabidopsis. *Plant J*, **70**, 831-844.
- Li, J., Zhang, J., Wang, X. and Chen, J.** (2010) A membrane-tethered transcription factor ANAC089 negatively regulates floral initiation in Arabidopsis thaliana. *Sci China Life Sci*, **53**, 1299-1306.
- Li, P., Zhou, H., Shi, X., Yu, B., Zhou, Y., Chen, S., Wang, Y., Peng, Y., Meyer, R.C., Smeekeens, S.C. and Teng, S.** (2014) The ABI4-induced Arabidopsis ANAC060 transcription factor attenuates ABA signaling and renders seedlings sugar insensitive when present in the nucleus. *PLoS Genet*, **10**, e1004213.
- Liang, C., Wang, Y., Zhu, Y., Tang, J., Hu, B., Liu, L., Ou, S., Wu, H., Sun, X., Chu, J. and Chu, C.** (2014) OsNAP connects abscisic acid and leaf senescence by fine-tuning abscisic acid biosynthesis and directly targeting senescence-associated genes in rice. *Proc Natl Acad Sci U S A*, **111**, 10013-10018.
- Liang, M., Li, H., Zhou, F., Li, H., Liu, J., Hao, Y., Wang, Y., Zhao, H. and Han, S.** (2015) Subcellular Distribution of NTL Transcription Factors in Arabidopsis thaliana. *Traffic*, **16**, 1062-1074.
- Lim, P.O., Kim, H.J. and Nam, H.G.** (2007) Leaf senescence. *Annu Rev Plant Biol*, **58**, 115-136.
- Lindemose, S., Jensen, M.K., Van de Velde, J., O'Shea, C., Heyndrickx, K.S., Workman, C.T., Vandepoele, K., Skriver, K. and De Masi, F.** (2014) A DNA-binding-site landscape and regulatory network analysis for NAC transcription factors in Arabidopsis thaliana. *Nucleic Acids Res*, **42**, 7681-7693.
- Ma, X., Zhang, Y., Tureckova, V., Xue, G.P., Fernie, A.R., Mueller-Roeber, B. and Balazadeh, S.** (2018) The NAC transcription factor SINAP2 regulates leaf senescence and fruit yield in Tomato. *Plant Physiol*, **177**, 1286-1302.
- Mahmood, K., El-Kereamy, A., Kim, S.H., Nambara, E. and Rothstein, S.J.** (2016) ANAC032 positively regulates age-dependent and stress-induced senescence in Arabidopsis thaliana. *Plant Cell Physiol*, **57**, 2029-2046.

- Mao, C., Lu, S., Lv, B., Zhang, B., Shen, J., He, J., Luo, L., Xi, D., Chen, X. and Ming, F. (2017) A Rice NAC transcription factor promotes leaf senescence via ABA biosynthesis. *Plant Physiol*, **174**, 1747-1763.
- Marino, D., Dunand, C., Puppo, A. and Pauly, N. (2012) A burst of plant NADPH oxidases. *Trends Plant Sci*, **17**, 9-15.
- Matallana-Ramirez, L.P., Rauf, M., Farage-Barhom, S., Dortay, H., Xue, G.P., Droge-Laser, W., Lers, A., Balazadeh, S. and Mueller-Roeber, B. (2013) NAC transcription factor ORE1 and senescence-induced bifunctional nuclease1 (BFN1) constitute a regulatory cascade in Arabidopsis. *Mol Plant*, **6**, 1432-1452.
- Mendes, G.C., Reis, P.A., Calil, I.P., Carvalho, H.H., Aragao, F.J. and Fontes, E.P. (2013) GmNAC30 and GmNAC81 integrate the endoplasmic reticulum stress- and osmotic stress-induced cell death responses through a vacuolar processing enzyme. *Proc Natl Acad Sci U S A*, **110**, 19627-19632.
- Mhamdi, A. and Van Breusegem, F. (2018) Reactive oxygen species in plant development. *Development*, **145**.
- Mittler, R. (2017) ROS are good. *Trends Plant Sci*, **22**, 11-19.
- Nelson, B.K., Cai, X. and Nebenfuhr, A. (2007) A multicolored set of in vivo organelle markers for co-localization studies in Arabidopsis and other plants. *Plant J*, **51**, 1126-1136.
- Ng, S., Ivanova, A., Duncan, O., Law, S.R., Van Aken, O., De Clercq, I., Wang, Y., Carrie, C., Xu, L., Kmiec, B., Walker, H., Van Breusegem, F., Whelan, J. and Giraud, E. (2013) A membrane-bound NAC transcription factor, ANAC017, mediates mitochondrial retrograde signaling in Arabidopsis. *Plant Cell*, **25**, 3450-3471.
- Oda-Yamamizo, C., Mitsuda, N., Sakamoto, S., Ogawa, D., Ohme-Takagi, M. and Ohmiya, A. (2016) The NAC transcription factor ANAC046 is a positive regulator of chlorophyll degradation and senescence in Arabidopsis leaves. *Sci Rep*, **6**, 23609.
- Olsen, A.N., Ernst, H.A., Leggio, L.L. and Skriver, K. (2005) NAC transcription factors: structurally distinct, functionally diverse. *Trends Plant Sci*, **10**, 79-87.
- Park, J., Kim, Y.S., Kim, S.G., Jung, J.H., Woo, J.C. and Park, C.M. (2011) Integration of auxin and salt signals by the NAC transcription factor NTM2 during seed germination in Arabidopsis. *Plant Physiol*, **156**, 537-549.
- Patterson, B.D., MacRae, E.A. and Ferguson, I.B. (1984) Estimation of hydrogen peroxide in plant extracts using titanium(IV). *Anal Biochem*, **139**, 487-492.
- Perez-Amador, M.A., Abler, M.L., De Rocher, E.J., Thompson, D.M., van Hoof, A., LeBrasseur, N.D., Lers, A.

- and Green, P.J.** (2000) Identification of BFN1, a bifunctional nuclease induced during leaf and stem senescence in Arabidopsis. *Plant Physiol*, **122**, 169-180.
- Pfaffl, M.W.** (2001) A new mathematical model for relative quantification in real-time RT-PCR. *Nucleic Acids Research*, **29**.
- Pimenta, M.R., Silva, P.A., Mendes, G.C., Alves, J.R., Caetano, H.D., Machado, J.P., Brustolini, O.J., Carpinetti, P.A., Melo, B.P., Silva, J.C., Rosado, G.L., Ferreira, M.F., Dal-Bianco, M., Picoli, E.A., Aragao, F.J., Ramos, H.J. and Fontes, E.P.** (2016) The stress-induced Soybean NAC transcription factor GmNAC81 plays a positive role in developmentally programmed leaf senescence. *Plant Cell Physiol*, **57**, 1098-1114.
- Pontier, D., Gan, S., Amasino, R.M., Roby, D. and Lam, E.** (1999) Markers for hypersensitive response and senescence show distinct patterns of expression. *Plant Mol Biol*, **39**, 1243-1255.
- Puranik, S., Sahu, P.P., Srivastava, P.S. and Prasad, M.** (2012) NAC proteins: regulation and role in stress tolerance. *Trends Plant Sci*, **17**, 369-381.
- Qiu, K., Li, Z., Yang, Z., Chen, J., Wu, S., Zhu, X., Gao, S., Gao, J., Ren, G., Kuai, B. and Zhou, X.** (2015) EIN3 and ORE1 accelerate degreening during ethylene-mediated leaf senescence by directly activating chlorophyll catabolic genes in Arabidopsis. *PLoS Genet*, **11**, e1005399.
- Rauf, M., Arif, M., Dortay, H., Matallana-Ramirez, L.P., Waters, M.T., Gil Nam, H., Lim, P.O., Mueller-Roeber, B. and Balazadeh, S.** (2013) ORE1 balances leaf senescence against maintenance by antagonizing G2-like-mediated transcription. *EMBO Rep*, **14**, 382-388.
- Rivero, R.M., Kojima, M., Gepstein, A., Sakakibara, H., Mittler, R., Gepstein, S. and Blumwald, E.** (2007) Delayed leaf senescence induces extreme drought tolerance in a flowering plant. *Proc Natl Acad Sci U S A*, **104**, 19631-19636.
- Rizhsky, L., Davletova, S., Liang, H. and Mittler, R.** (2004) The zinc finger protein Zat12 is required for cytosolic ascorbate peroxidase 1 expression during oxidative stress in Arabidopsis. *J Biol Chem*, **279**, 11736-11743.
- Rogers, H. and Munne-Bosch, S.** (2016) Production and scavenging of reactive oxygen species and redox signaling during leaf and flower senescence: similar but different. *Plant Physiol*, **171**, 1560-1568.
- Sakuraba, Y., Han, S.H., Lee, S.H., Hortensteiner, S. and Paek, N.C.** (2016) Arabidopsis NAC016 promotes chlorophyll breakdown by directly upregulating STAYGREEN1 transcription. *Plant Cell Rep*, **35**, 155-166.

- Sakuraba, Y., Kim, Y.S., Han, S.H., Lee, B.D. and Paek, N.C.** (2015) The Arabidopsis transcription factor NAC016 promotes drought stress responses by repressing AREB1 transcription through a trifurcate feed-forward regulatory loop involving NAP. *Plant Cell*, **27**, 1771-1787.
- Saleh, A., Alvarez-Venegas, R. and Avramova, Z.** (2008) An efficient chromatin immunoprecipitation (ChIP) protocol for studying histone modifications in Arabidopsis plants. *Nat Protoc*, **3**, 1018-1025.
- Sato, Y., Morita, R., Katsuma, S., Nishimura, M., Tanaka, A. and Kusaba, M.** (2009) Two short-chain dehydrogenase/reductases, NON-YELLOW COLORING 1 and NYC1-LIKE, are required for chlorophyll b and light-harvesting complex II degradation during senescence in rice. *Plant Journal*, **57**, 120-131.
- Seo, P.J., Kim, M.J., Park, J.Y., Kim, S.Y., Jeon, J., Lee, Y.H., Kim, J. and Park, C.M.** (2010) Cold activation of a plasma membrane-tethered NAC transcription factor induces a pathogen resistance response in Arabidopsis. *Plant J*, **61**, 661-671.
- Seo, P.J., Kim, S.G. and Park, C.M.** (2008) Membrane-bound transcription factors in plants. *Trends Plant Sci*, **13**, 550-556.
- Seo, P.J., Park, J.M., Kang, S.K., Kim, S.G. and Park, C.M.** (2011) An Arabidopsis senescence-associated protein SAG29 regulates cell viability under high salinity. *Planta*, **233**, 189-200.
- Sun, Y., Wang, C., Yang, B., Wu, F., Hao, X., Liang, W., Niu, F., Yan, J., Zhang, H., Wang, B., Deyholos, M.K. and Jiang, Y.Q.** (2014) Identification and functional analysis of mitogen-activated protein kinase kinase (MAPKKK) genes in canola (*Brassica napus* L.). *J Exp Bot*, **65**, 2171-2188.
- Suzuki, N., Miller, G., Morales, J., Shulaev, V., Torres, M.A. and Mittler, R.** (2011) Respiratory burst oxidases: the engines of ROS signaling. *Curr Opin Plant Biol*, **14**, 691-699.
- Thomas, H.** (2013) Senescence, ageing and death of the whole plant. *New Phytol.*, **197**, 696-711.
- Torres, M.A., Dangl, J.L. and Jones, J.D.** (2002) Arabidopsis gp91phox homologues AtrbohD and AtrbohF are required for accumulation of reactive oxygen intermediates in the plant defense response. *Proc Natl Acad Sci USA*, **99**, 517-522.
- Uauy, C., Distelfeld, A., Fahima, T., Blechl, A. and Dubcovsky, J.** (2006) A NAC gene regulating senescence improves grain protein, zinc, and iron content in wheat. *Science*, **314**, 1298-1301.
- Van Aken, O. and Pogson, B.J.** (2017) Convergence of mitochondrial and chloroplastic ANAC017/PAP-dependent retrograde signalling pathways and suppression of programmed cell death. *Cell Death Differ*, **24**, 955-960.

- Wang, B., Guo, X., Wang, C., Ma, J., Niu, F., Zhang, H., Yang, B., Liang, W., Han, F. and Jiang, Y.Q. (2015) Identification and characterization of plant-specific NAC gene family in canola (*Brassica napus* L.) reveal novel members involved in cell death. *Plant Mol Biol*, **87**, 395-411.
- Waters, M.T., Moylan, E.C. and Langdale, J.A. (2008) GLK transcription factors regulate chloroplast development in a cell-autonomous manner. *Plant J*, **56**, 432-444.
- Weaver, L.M., Gan, S., Quirino, B. and Amasino, R.M. (1998) A comparison of the expression patterns of several senescence-associated genes in response to stress and hormone treatment. *Plant Mol. Biol.*, **37**, 455-469.
- Woo, H.R., Kim, H.J., Nam, H.G. and Lim, P.O. (2013) Plant leaf senescence and death - regulation by multiple layers of control and implications for aging in general. *J Cell Sci*, **126**, 4823-4833.
- Woo, H.R., Koo, H.J., Kim, J., Jeong, H., Yang, J.O., Lee, I.H., Jun, J.H., Choi, S.H., Park, S.J., Kang, B., Kim, Y.W., Phee, B.K., Kim, J.H., Seo, C., Park, C., Kim, S.C., Park, S., Lee, B., Lee, S., Hwang, D., Nam, H.G. and Lim, P.O. (2016) Programming of plant leaf senescence with temporal and inter-organellar coordination of transcriptome in *Arabidopsis*. *Plant Physiol.*, **171**, 452-467.
- Wu, A., Allu, A.D., Garapati, P., Siddiqui, H., Dortay, H., Zanol, M.I., Asensi-Fabado, M.A., Munne-Bosch, S., Antonio, C., Tohge, T., Fernie, A.R., Kaufmann, K., Xue, G.P., Mueller-Roeber, B. and Balazadeh, S. (2012) JUNGBRUNNEN1, a reactive oxygen species-responsive NAC transcription factor, regulates longevity in *Arabidopsis*. *Plant Cell*, **24**, 482-506.
- Yan, J., Tong, T., Li, X., Chen, Q., Dai, M., Niu, F., Yang, M., Deyholos, M.K., Yang, B. and Jiang, Y.Q. (2018) A novel NAC-type transcription factor, NAC87, from oilseed rape modulates reactive oxygen species accumulation and cell death. *Plant Cell Physiol*, **59**, 290-303.
- Yang, L., Ye, C., Zhao, Y., Cheng, X., Wang, Y., Jiang, Y.Q. and Yang, B. (2018) An oilseed rape WRKY-type transcription factor regulates ROS accumulation and leaf senescence in *Nicotiana benthamiana* and *Arabidopsis* through modulating transcription of RbohD and RbohF. *Planta*, **247**, 1323-1338.
- Yang, S.D., Seo, P.J., Yoon, H.K. and Park, C.M. (2011) The *Arabidopsis* NAC transcription factor VNI2 integrates abscisic acid signals into leaf senescence via the COR/RD genes. *Plant Cell*, **23**, 2155-2168.
- Yang, Z.T., Lu, S.J., Wang, M.J., Bi, D.L., Sun, L., Zhou, S.F., Song, Z.T. and Liu, J.X. (2014a) A plasma membrane-tethered transcription factor, NAC062/ANAC062/NTL6, mediates the unfolded protein response in *Arabidopsis*. *Plant J*, **79**, 1033-1043.

Yang, Z.T., Wang, M.J., Sun, L., Lu, S.J., Bi, D.L., Sun, L., Song, Z.T., Zhang, S.S., Zhou, S.F. and Liu, J.X.

(2014b) The membrane-associated transcription factor NAC089 controls ER-stress-induced programmed cell death in plants. *PLoS Genet*, **10**, e1004243.

Yoo, S.D., Cho, Y.H. and Sheen, J. (2007) Arabidopsis mesophyll protoplasts: a versatile cell system for transient gene expression analysis. *Nat Protoc*, **2**, 1565-1572.

Zhang, D., Liu, D., Lv, X., Wang, Y., Xun, Z., Liu, Z., Li, F. and Lu, H. (2014) The cysteine protease CEP1, a key executor involved in tapetal programmed cell death, regulates pollen development in Arabidopsis. *Plant Cell*, **26**, 2939-2961.

Zhang, K. and Gan, S.S. (2012) An abscisic acid-AtNAP transcription factor-SAG113 protein phosphatase 2C regulatory chain for controlling dehydration in senescing Arabidopsis leaves. *Plant Physiol*, **158**, 961-969.

Zheng, M.S., Takahashi, H., Miyazaki, A., Hamamoto, H., Shah, J., Yamaguchi, I. and Kusano, T. (2004) Up-regulation of Arabidopsis thaliana NHL10 in the hypersensitive response to Cucumber mosaic virus infection and in senescing leaves is controlled by signalling pathways that differ in salicylate involvement. *Planta*, **218**, 740-750.

Zhu, X., Chen, J., Xie, Z., Gao, J., Ren, G., Gao, S., Zhou, X. and Kuai, B. (2015) Jasmonic acid promotes degreening via MYC2/3/4- and ANAC019/055/072-mediated regulation of major chlorophyll catabolic genes. *Plant J*, **84**, 597-610.

Figures and figure legends:

Figure 1. Subcellular localization of BnaNAC60 and expression analysis of *BnaNAC60*. (a) Schematic representation of BnaNAC60 protein. The N-terminus contains a conserved NAC domain which can be divided into five subdomains and has DNA binding ability. The C-terminus has transcriptional regulatory ability and contains a transmembrane domain. BnaNAC60 Δ TM is a truncated form without the transmembrane domain. (b) Subcellular localization of BnaNAC60 and its truncated form by transient expression in *N.benthamiana* cells. The GFP-BnaNAC60 and GFP-BnaNAC60 Δ TM fusion proteins were co-localized with the mCherry-tagged HDEL or the NLS. Bar, 50 μ m. (c) Expression level of *BnaNAC60* determined by qRT-PCR during leaf development in oilseed rape. The fourth true leaves of oilseed rape at different developmental stages were used for the assay. YL, young leaves; ML, mature leaves; ES, early senescent leaves; LS, late senescent leaves; T, M, B are the tip, middle and base of ES leaves. (d) Expression of *BnaNAC60* upon various treatments including 50 μ M (\pm)-ABA, 2 mM salicylic acid (SA), 50 μ M jasmonate (JA), 10 μ M methyl viologen (MV), 20 mM H₂O₂, 15% PEG8000, 200 mM NaCl, heat (38°C) and cold (4°C). In (c) and (d), data represent means of three biological replicates \pm SE compared to YL (c) or mock treatment (d). Asterisks indicate significant differences by Student's *t*-test (* $P \leq 0.05$; ** $P \leq 0.01$).

Figure 2. Overexpression of *BnaNAC60* Δ TM in Arabidopsis promotes age-dependent leaf senescence. (a) Phenotype of two *BnaNAC60* Δ TM-overexpression lines OE-31# and OE-28# compared to the transgenic *GFP* control line. Photographs were taken at 40 dps (days post-stratification) and the 5th to 8th true leaves were stained with DAB (3,3'-diaminobenzidine).

Bar, 1 cm. (b), (c) and (d) Quantification of H₂O₂ (b), chlorophyll (c) and relative conductivity (d) contents in these two OE lines compared with the control line. Values represent the means of three independent replicates \pm SE. Asterisks indicate the significant difference compared to *GFP* control line by Student's *t*-test (* $P \leq 0.05$; ** $P \leq 0.01$). (e) qRT-PCR analysis of the expression of senescence-, ROS- and cell death-related marker genes in these two OE lines at 40 dps. The age-matched plants of *GFP* line was used as the control. Data are mean of three replicates \pm SE. Asterisks indicate the significant difference compared to expression levels in the *GFP* control line, by Student's *t*-test (* $P \leq 0.05$; ** $P \leq 0.01$).

Figure 3. *BnaNAC60* expression induced ROS accumulation and cell death in oilseed rape protoplasts. (a) Examination of cell death by Evans blue staining. Arrows represent dead protoplasts stained by Evans blue dye. Bars, 50 μ m. (b) FDA staining to investigate the cell viability. Bars, 100 μ m. Arrows indicate dead protoplasts. Autofluorescence of chloroplasts was shown in the 2nd last panel in both (a) and (b). (c)-(d) Percentages of dead protoplasts as detected by Evans blue and FDA stainings in (a) and (b), respectively. Data are mean of three replicates \pm SE (n = 20). Asterisks indicate significant differences by Student's *t*-test (* $P \leq 0.05$; ** $P \leq 0.01$). (e) Detection of ROS level through the fluorescent H₂DCFDA dye. The green fluorescence indicates the production of ROS. Bars, 50 μ m.

Figure 4. Identification the binding motif of *BnaNAC60* and expression analysis of marker genes. (a) A schematic diagram showing the double reporter and effector plasmids. The double reporter plasmid contains the synthetic 5xNTLBS elements fused to the minimal promoter sequence of CaMV35S inserted upstream of *LUC* reporter gene. The *Renilla luciferase* (*REN*) driven by CaMV35S included in the same construct served for internal normalization. The effector plasmid contains *BnaNAC60* or its truncated form *BnaNAC60 Δ TM* driven by CaMV35S. *GUS* expression plasmid was used the control effector. TL, translational leader sequence; Ter, transcriptional termination sequence. (b) A dual luciferase assay of *BnaNAC60*-mediated transactivation of *LUC* reporter gene driven by 5xNTLBS-35Smin promoter in *N.benthamiana* leaves. Ratios of LUC to

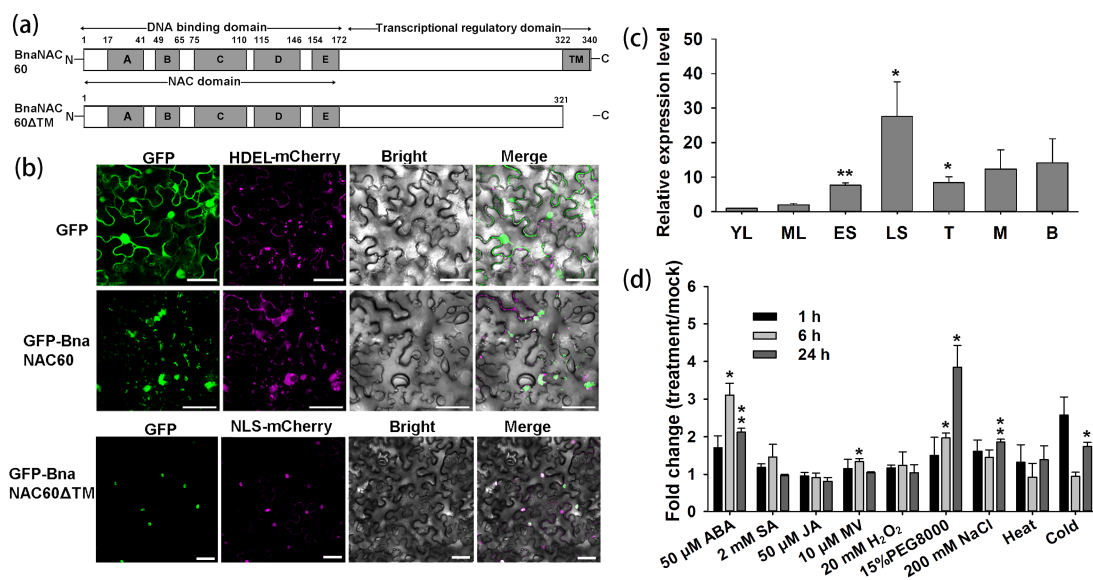
REN activities were used to reflect the transcriptional ability. Asterisks indicate significant differences by Student's *t*-test (** $P \leq 0.01$). (c) Electrophoretic mobility shift assay (EMSA) of BnaNAC60 Δ TM binding to the 5xNTLBS element labeled with biotin. The GST-BnaNAC60 Δ TM fusion protein was used to detect its binding ability to 5xNTLBS and the GST protein was used as a negative control. Competitor (unlabelled probes) was used in molar excess. The bands in the upper and lower panel indicate shift (protein-DNA complex) and unbound free probes, respectively. (d) Transcript abundance analysis of ROS-, cell death-, senescence- and defense-related marker genes in cotyledons of oilseed rape transiently expressing BnaNAC60 and BnaNAC60 Δ TM. Transcript levels were measured at two time points (1 and 2 dpi). GFP-expression tissues were used as the control. Data represent the geometric mean \pm SE of three biological replicates. The BnaUPI and BnaUBC9 genes were used as the endogenous references. Asterisks indicate the significant difference compared to GFP-expressing tissue by Student's *t*-test (* $P \leq 0.05$; ** $P \leq 0.01$).

Figure 5. The dual luciferase reporter assay of transcriptional activation of putative target genes by BnaNAC60. (a) A schematic diagram of the double reporter and effector plasmids. LUC and REN represent firefly luciferase and *Renilla* luciferase, respectively. pYJHA-GUS plasmid was used the control effector. Ter, terminator sequence of transcription. (b-i) Examination of BnaNAC60 and BnaNAC60 Δ TM ability to activate the transcription of *LUC* reporter gene under the control of different promoter regions of marker genes from oilseed rape. Relative reporter activity was normalized by the ratio of LUC/REN. Data were from three independent replicates \pm SE at two time points. dpi, days post-infiltration. Asterisks indicate the significant difference compared to GUS effector by Student's *t*-test (* $P \leq 0.05$; ** $P \leq 0.01$).

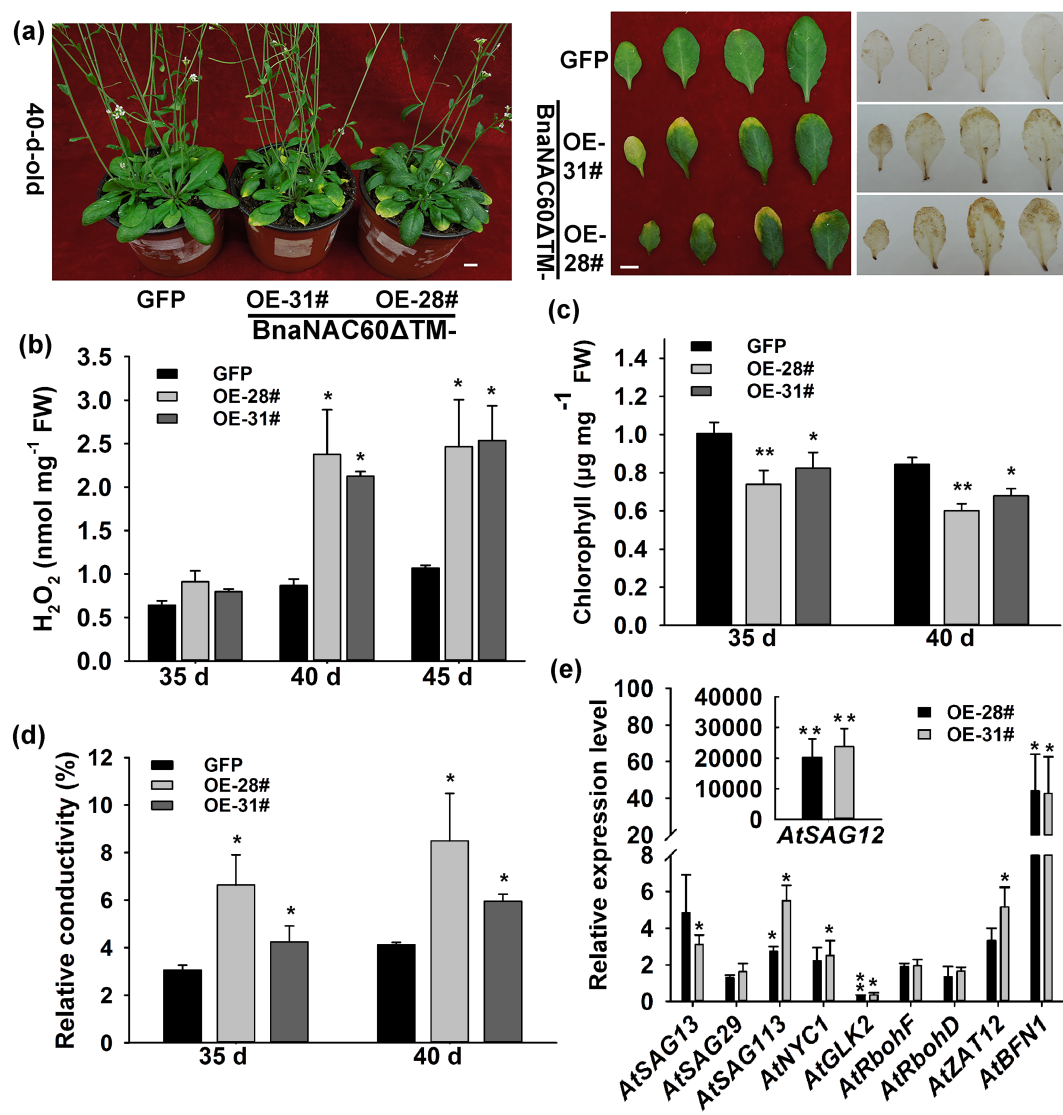
Figure 6. Electrophoretic mobility shift assay (EMSA) of BnaNAC60 Δ TM binding to different fragments in the promoter regions of putative target genes. (a) Schematic diagrams of NTLBS elements in the promoters of putative target genes. White and black diamonds indicate the binding elements on sense and anti-sense strands, respectively. The promoter lengths and sites of NTLBS

elements are drawn in scale. Fxs represent the fragments tested by EMSA. ATG is the translational start codon. (b) Assay of GST-BnaNAC60ΔTM fusion protein binding to different biotin-labeled fragments of promoter regions of putative target genes. GST protein was used as a negative control. Competitor probes (unlabeled) were added in molar excess as shown above the images. “+” and “-” represent presence and absence of one component in binding reactions, respectively. Shifts indicate the protein-DNA complex while free probes mean unbound probes.

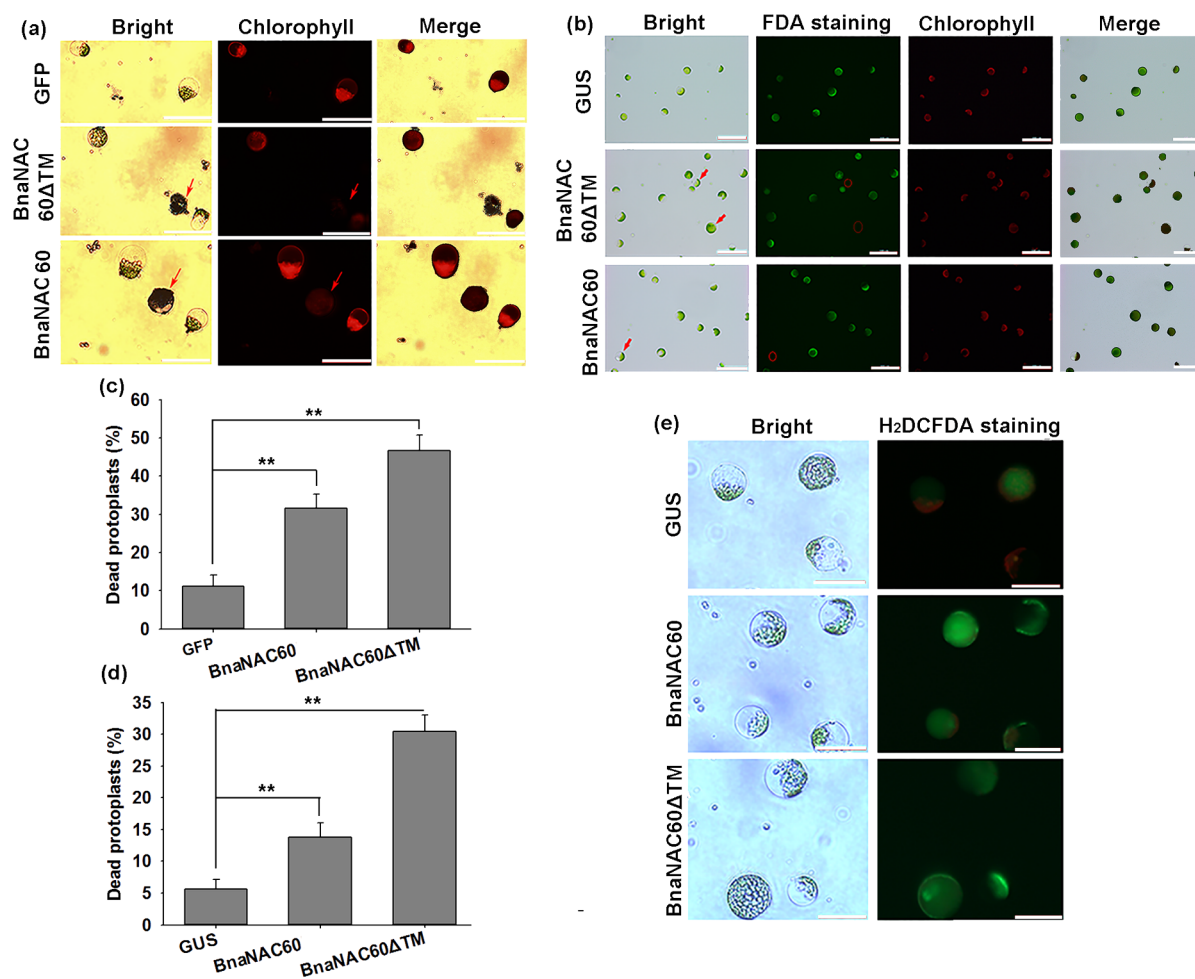
Figure 7. ChIP-qPCR assay of binding of BnaNAC60ΔTM to the promoter regions of target genes in oilseed rape. (a) Schematic representation of NTLBS elements in promoter regions of target genes. ATG, translational start codon. The diamonds indicate the NTLBS binding elements. The thin black bars indicated by Pxs above the promoters represent regions which were amplified in qPCR and the numbers show the distance (in bp) from ATG start codon. CK, genomic control regions amplified in qPCR in parallel. (b) ChIP-qPCR results. Chromatin DNA was co-immunoprecipitated with anti-HA antibody or no antibody. Fragmented genomic DNA was released from the protein-DNA complexes and subjected to qPCR analysis. Input sample was used to normalize the qPCR results in each ChIP sample. Data are mean ± SE of three biological replicates. Asterisks indicate the significant difference by Student's *t*-test (* $P \leq 0.05$; ** $P \leq 0.01$).



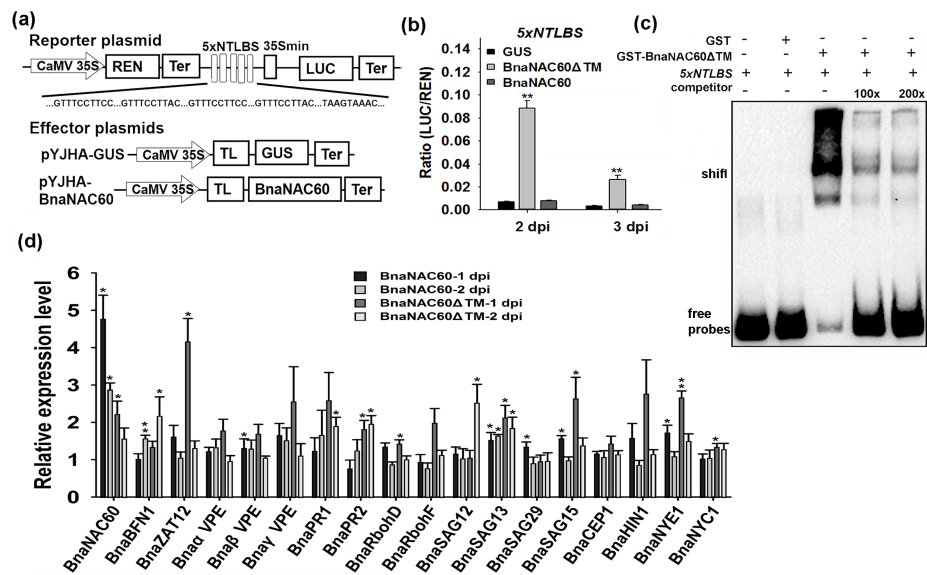
tpj_15057_f1.tiff



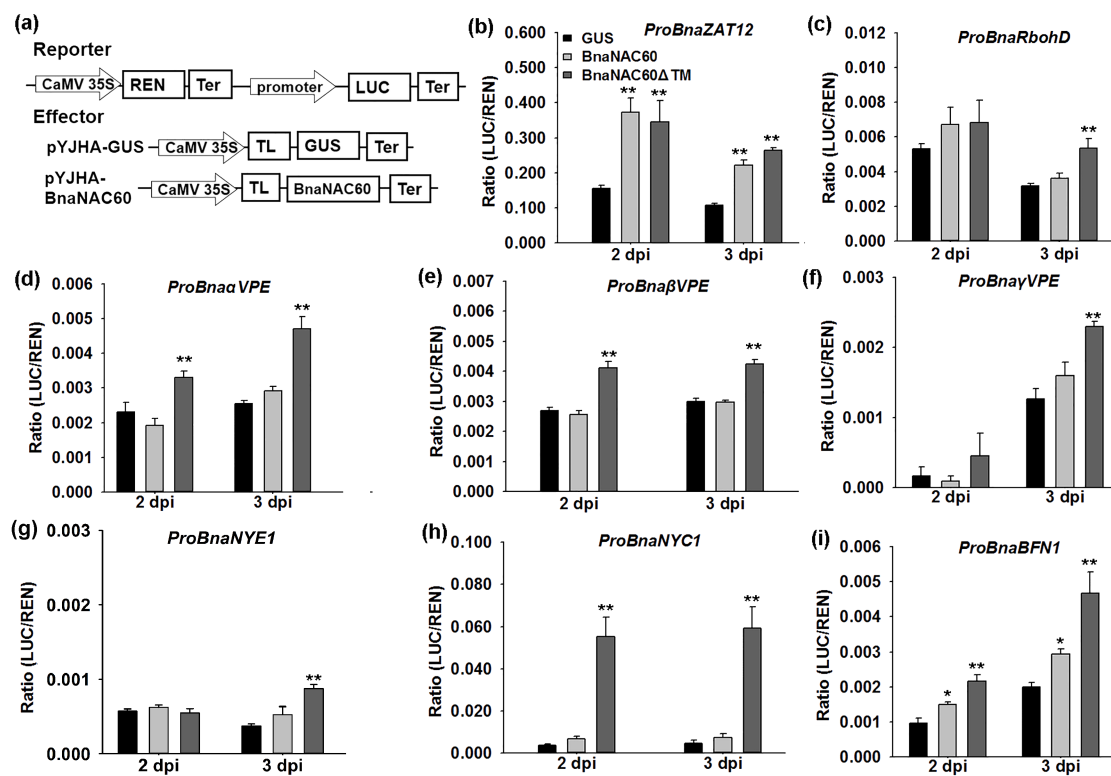
tpj_15057_f2.tiff



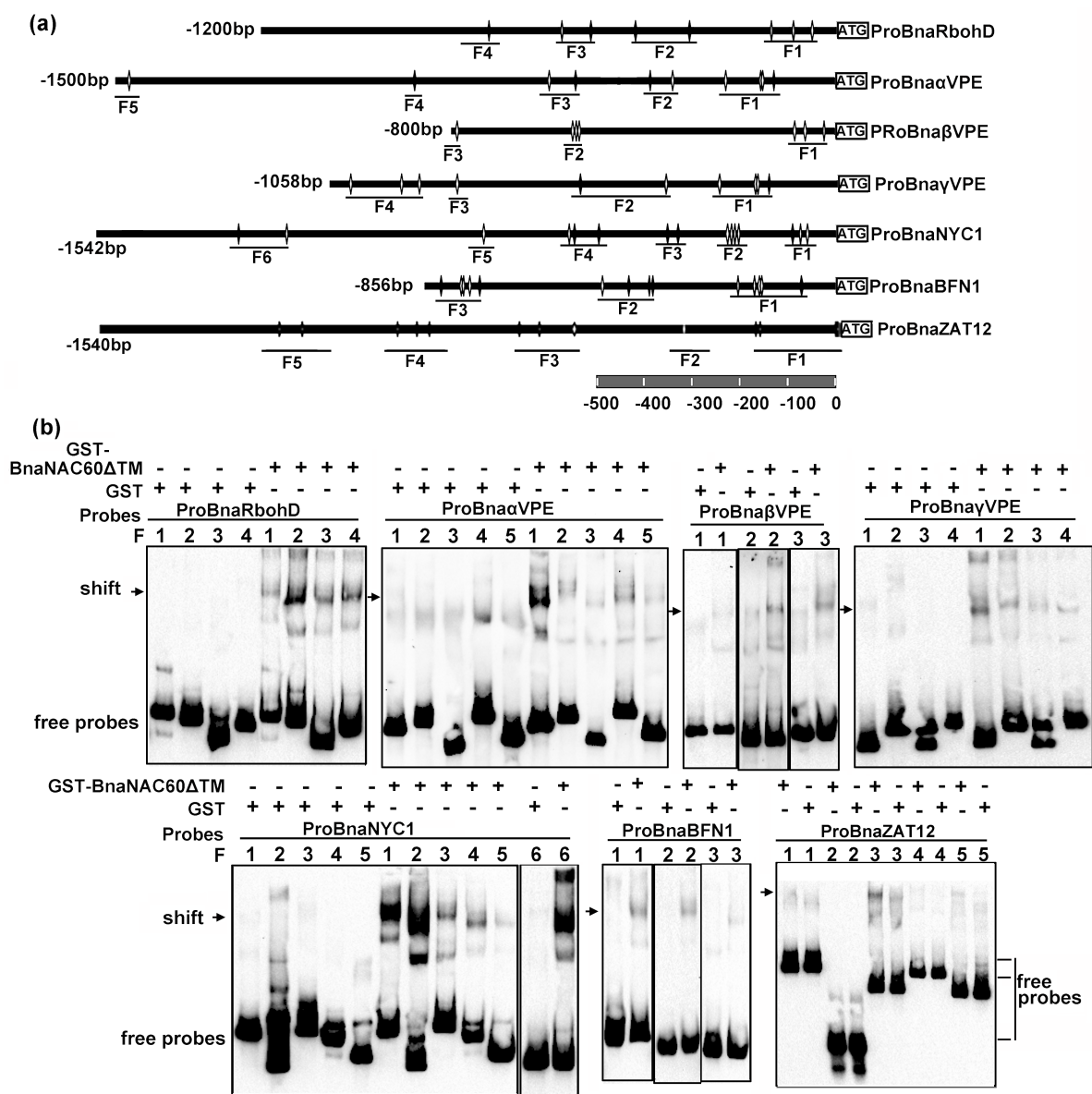
tpj_15057_f3.tiff

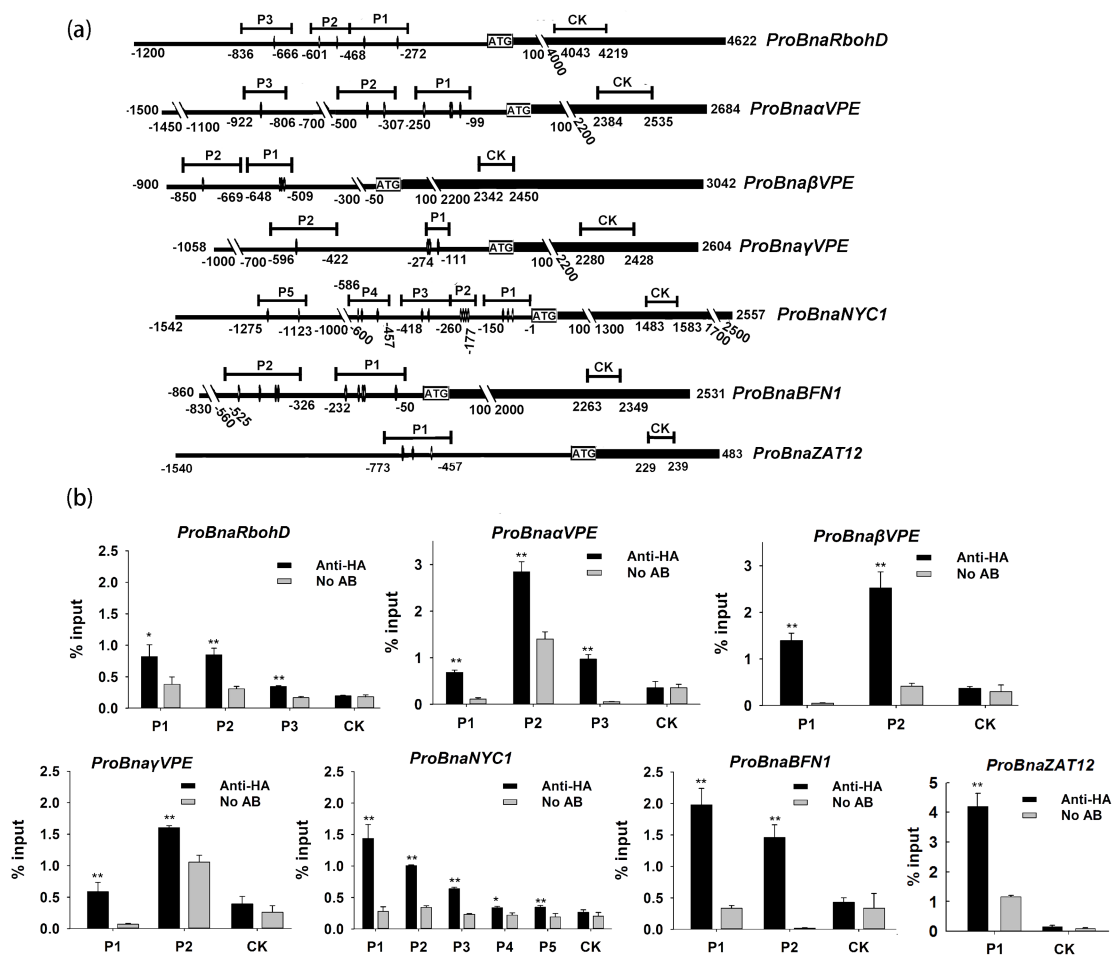


tpj_15057_f4.tiff



tpj_15057_f5.tiff





tpj_15057_f7.tif